Dose-dependency of heterochromatin domains reveals subtelomeric structuration in budding yeast

Antoine Hocher[1,2], Myriam Ruault[1,2], Marc Descrimes[1,2], Mickael Garnier[1,2], Antonin Morillon[1,2], Angela Taddei[1,2]

Affiliations:

[1] Institut Curie, PSL Research University, CNRS, UMR3664, F-75005 Paris, France

[2] Sorbonne Universités, UPMC Univ Paris 06, CNRS, UMR3664, F-75005 Paris, France

Abstract

The eukaryotic genome is divided into chromosomal domains of distinct gene activities. Transcriptionally silent chromatin is found in subtelomeric regions leading to telomeric position effect (TPE) in yeast, fly and man. Silent chromatin generally initiates at defined loci and tends to propagate from those sites by self-recruitment mechanisms implying the requirement for processes preventing ectopic spreading of silencing. Barrier elements that can block the spread of silent chromatin have been documented, but their relative efficiency is not known.

Here we explore the dose-dependency of silencing factors for the extent of TPE in budding yeast. We characterized genome widely the impact of overexpressing the silencing factors Sir2 and Sir3 on the spreading of Sir3 and its impact on coding and non-coding transcription. We thus reveal that extension of silent domains can reach saturation. Analysis of published data sets enabled to uncover that the extension of Sir3 bound domains stops at zones corresponding to transitions of specific histone marks including H3K79 methylation that is deposited by the conserved enzyme Dot1. Importantly, *DOT1* is essential for viability when Sir3 is in excess indicating that this transition actively blocks Sir3 spreading. Our work uncovers previously uncharacterized discrete chromosomal domains associated with specific chromatin features and demonstrates that TPE is efficiently restricted to subtelomeres by the preexisting chromatin landscape.

Introduction

Heterochromatin classically designates chromosomal domains that remain condensed throughout the cell cycle (Heitz, E 1928). It impacts many aspects of chromosome biology including genomic stability and gene expression (Grewal and Jia 2007). In opposition to gene specific repressors, heterochromatin based regulation of transcription allows the silencing of genes independently of DNA sequence (Talbert and Henikoff 2006). Its prevalence in eukaryotic genomes makes heterochromatin a major system of gene regulation, key to processes ranging from gene dosage to differentiation and speciation (Grewal and Jia 2007). Silencing generally initiates at defined loci and tends to propagate from those sites by self-recruitment mechanisms (Grunstein 1997; Hoppe et al. 2002). The coupling of histone modifying enzymes to the specific association of silencing effector with nucleosomes drives the formation of regional domains of heterochromatin (L N Rusche, Kirchmaier, and Rine 2002). However, this potent mechanism comes at a price and requires the establishment of mechanisms to limits the ectopic spread of heterochromatin (David Donze and Kamakaka 2002). Albeit punctual barrier elements have been shown to block the spread of heterochromatin, the mechanism underlying those process remains elusive.

In budding yeast, a similar system of epigenetic silencing is found at the silent mating type loci (HML and HMR), at subtelomeres and within the ribosomal DNA array. Silencing at the ribosomal DNA array involves the RENT complex, while the silent information regulator (SIR) proteins, Sir2 Sir3 and Sir4, implement stable repression of mating type loci and semi-stable repression of genes at the vicinity of telomeres (Gartenberg and Smith 2016; Grunstein and Gasser 2013; Aparicio, Billington, and Gottschling 1991; Moazed et al. 1997; Rine and Herskowitz 1987; Rudner et al. 2005; Laura N Rusche, Kirchmaier, and Rine 2003).

Sir2/Sir4 heterodimers and Sir3 are recruited at the HM through interaction with Orc1-bound Sir1 and Rap1 (Hoppe et al. 2002; Luo, Vega-Palas, and Grunstein 2002; Paolo Moretti et al. 1994; P Moretti and Shore 2001; L N Rusche, Kirchmaier, and Rine 2002; Triolo and Sternglanz 1996). At telomeres, interactions of Sir3 and Sir2/Sir4 with Rap1p arrays are sufficient to nucleate silencing (Marcand et al. 1996). Additional interaction of Sir4 with the Ku heterodimers reinforces silencing (Tsukamoto, Kato, and Ikeda 1997; Roy et al. 2004)

Once nucleated, the activity of Sir2, a conserved NAD+ dependent histone deacetylase, creates favorable binding sites for Sir3. The bromo-adjacent-homology (BAH) domain of Sir3 drives the selectivity of Sir3 association with nucleosomes. Crystal studies and genetics evidences demonstrated that Sir3 preferentially binds nucleosomes unmodified at H3K79 and at H4K16. Iterative cycles of histone modification and binding allow the self-propagation of the SIR complex on chromatin until a barrier is eventually reached(Grunstein and Gasser 2013; Gartenberg and Smith 2016).

Boundaries restrict silent domains at the mating type loci (David Donze et al. 1999; D. Donze and Kamakaka 2001). A tRNA confines the Sir complex to HMR (David Donze et al. 1999) while directional nucleation restricts HML silencing (X Bi et al. 1999). In contrast subtelomeric silencing is rather constrained than restricted. The collective action of chromatin modifying enzymes implements chromatin states that potentially decrease Sir3 affinity for nucleosomes. In addition to the acetylation of H4K16 by the SAS-I complex, acetylation of histone H3 tails by Gcn5 and Elp3, methylation of H3K4 and H3K79 residues and H4K16ac dependent incorporation of the H2A.Z histone variant were all proposed to contribute to the instable equilibrium ruling Sir3 propagation at subtelomeres(Gartenberg and Smith 2016) .

In mutants lacking those enzymes the SIR complex propagates further away from the telomeres. However the respective contribution of each mechanism and what further limits silencing spreading in those mutants remains unknown. In addition numerous factors have been identified on the basis of their barrier properties using boundary assays, which consists in targeting candidate factors fused to a DNA binding domain between a silencer and a reporter gene, but their role *in vivo* remains to be explored (Oki et al. 2004). This is the case for nuclear pore complex components or transcription factors.

A key parameter regulating heterochromatin dynamics is the concentration of silencing factors. In *S.pombe* increasing the dosage of the silencing factor Swi6, bypasses the need for the RNA interference machinery at centromeric regions(Tadeo et al. 2013). In *S.pombe* and *S.cerevisiae*, increasing the level of Swi6 or Sir3 stabilizes variegation toward transcriptionally OFF states (Renauld et al. 1993a; Nakayama, Klar, and Grewal 2000). Importantly, silencing factors also influence the spatial distribution of heterochromatin,

S.pombe RNAi machinery and *S.cerevisiae* Sir complex being required for telomere clustering (Jia, Noma, and Grewal 2004; Guidi et al. 2015; Ruault et al. 2011a; Gotta et al. 1996). In budding yeast, SIR protein concentration is limiting silencing in wild type cells (Maillet et al. 1996; Renauld et al. 1993b). SIR proteins are unevenly distributed in the nucleus (Gotta et al. 1996). In cycling cells, the clustering of the 32 telomeres in discrete foci leads to the sequestration of SIR proteins at the nuclear periphery favoring SIR mediated repression in this subnuclear regions and preventing promiscuous repression elsewhere in the nucleus (Thompson, Johnson, and Grunstein 1994; Gotta et al. 1996; Andrulis et al. 1998; Taddei et al. 2009).

Furthermore, increasing Sir3 dosage in budding yeast leads to further expansion of silent domains toward the chromosome core (Renauld et al. 1993a) and to a concomitant increase of telomere clustering (Ruault et al., 2011). However, the dose-dependency of heterochromatin propagation is largely unknown. In this work we explore the consequences of controlled increases in Sir protein dosage genome wide. We show that saturating the levels of silencing effectors unveils the maximal extend of heterochromatin domains revealing discrete subtelomeric domains. Analysis of published data set in combination with ours revealed that these domains are characterized by the absence of H3 tri-methylation at lysine 4, 36 and 79 and the presence of H2A phosphorylation. Our study demonstrates that histone marks are a major factor restraining the spread of heterochromatin. In particular, our results points to a particular role of the tri-methylation of H3K79 in genome protection against silencing.

Results

Dose-dependency of telomere clustering and Sir3 spreading upon Sir3 overexpression.

To systemically examine the impact of high doses of Sir3 on the genome, we compared strains stably over-expressing *SIR3* at different levels. To minimize the cell-to-cell variability of Sir3 amounts, we replaced *SIR3* endogenous promoter by three different constructs (pADH, pTEF and pGPD) (Janke et al. 2004). We measured Sir3p levels by western blot (SupFigS1A), and by fluorescence quantification at the single cell level (Fig1A) in live cells expressing Sir3-GFP (SupFigS1B). Using this system, we measured telomere clustering and genome wide binding of Sir3p in strains producing 1x (WT), 9x (pADH-SIR3), 16x (pTEF-SIR3),

and 29x (pGPD-SIR3) Sir3p, with minor overlap in Sir3p levels between strains. Potential confounding effects due to differences in the cell cycle were excluded, FACS profiles of WT and pGPD-SIR3 strains being largely similar (SupFigS1D).

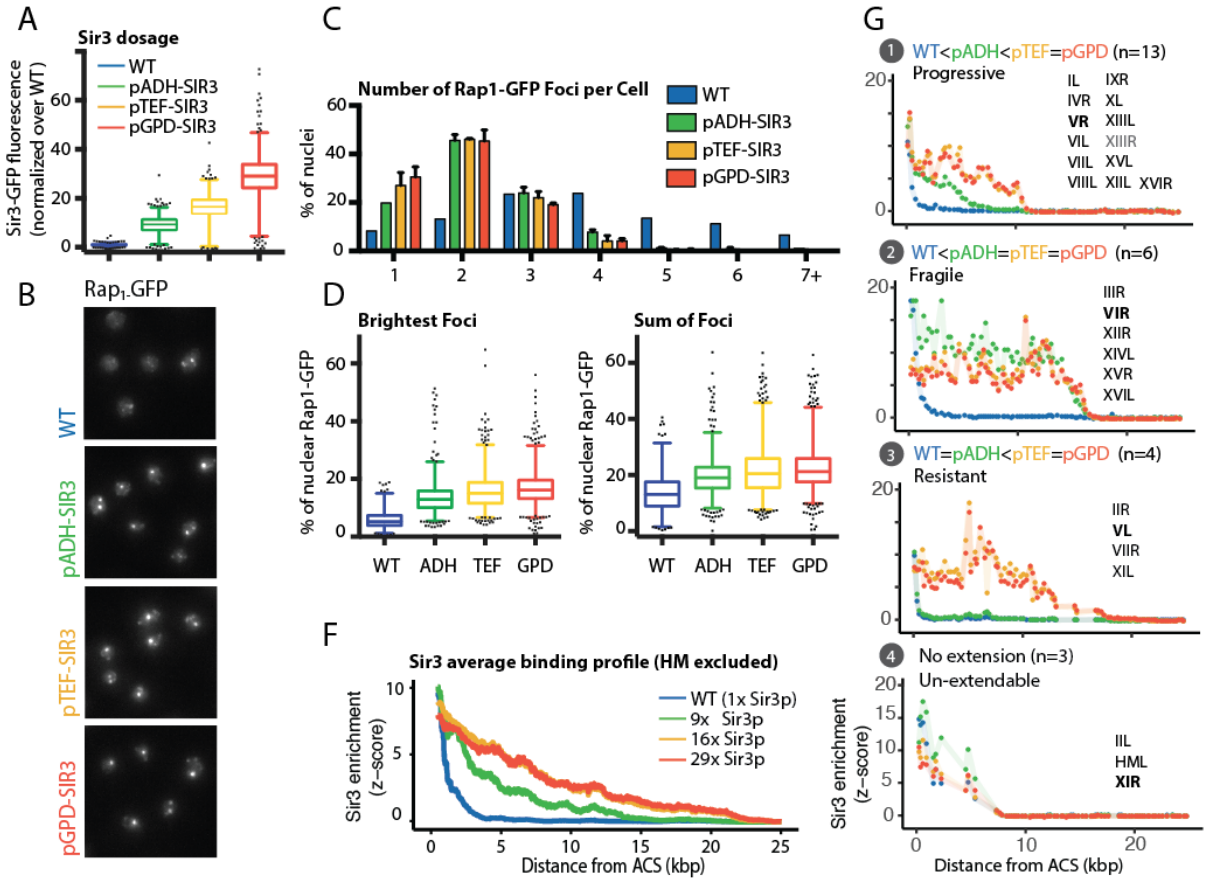

Figure 1 Increasing Sir3 dosage leads to telomere clustering and SIR spreading saturation. (A) Quantification of Sir3 levels by integration of Sir3-GFP signal in strains expressing SIR3-GFP (B) Rap1-GFP foci grouping in strain differing for Sir3 levels. Cells were grown in YPD overnight, diluted to OD600nm= 0.2, and imaged at OD600nm= 1. (C) Quantification of Rap1-GFP foci distribution in images from A. (D) left: Distribution of Rap1-GFP signal attributed to the brightest foci in each nucleus. (E) Distribution of the relative amount of Rap1 measured within foci relative to total nuclear Rap1 signal. (F) ChIP-chip against Sir3 was carried in strains from A. Moving average of Sir3 binding (block = 1000 bp, window = 10) at telomeres (with the exception of TELIIIL and TELIIIR which contain HM loci) as a function of distance from telomeric X core sequence. Enrichment is measured as the standardized IP over Input (See mat meth). (G) Stereotypical examples of Sir3 binding in function of Sir3 dosage, numbers correspond to the subtelomeres constituting each group, in bold is the subtelomere plotted.

We monitored telomere foci in function of Sir3 concentration by live microscopy imaging of Rap1-GFP (Fig1B). In the range of concentration probed, we observed that telomere clustering increase non-linearly in function of Sir3 levels.

Consistent with previous studies telomeres clustered into 2 to 6 foci in WT cells. Above 9x, changes in Sir3 concentration only had subtle effect and telomeres clustered within 1 to 3 foci, a configuration compatible with our previous observations (Fig1C). We reasoned that despite changes in the distribution of foci, the total fluorescence corresponding to Rap1-GFP foci would be conserved if all the telomeres were detected in wild type cells. To test this hypothesis, we summed the fluorescence within foci for each nucleus independently of the number of foci (Fig1C). We found that the proportion of nuclear Rap1-GFP increases from 13.6% in WT cells to a maximum of 21.6-22.2 % for Sir3 dosage above 16x. We did not detect significant differences between the proportions of Rap1 in foci in cells overexpressing 16x or 29x Sir3p (Holm-Sidak's multiple comparisons test). Thus at a given time only a fraction of telomeres are present in a telomeric foci visible by fluorescent microscopy. On average, the brightest focus of a wild type cell concentrated 5.6% of nuclear Rap1, significantly (p-value <0.0001, Holm-Sidak's multiple comparisons test) less than the brightest focus of a 9x, 16x or 29x Sir3 typical nuclei, which respectively accounts for 13.6, 16 and 16.8% of nuclear Rap1. The last differences being detected with low significance (p-value 0.0038).

Increase in foci intensity thus parallels the decrease in number of foci, which is consistent with an increase in telomere grouping in cells overexpressing Sir3. Telomere clustering reaches a maximum for Sir3 levels superior to 9 and inferior to 16 fold over WT.

In parallel, we probed genome-wide Sir3 binding in function of its dosage by chromatin immuno-precipitation analysed on chip (ChIP-Chip). In wild type cells, Sir3 binding was detected until ~5 kb away from the telomeric repeats on average, consistent with previous studies. Upon 9 fold increase of Sir3p, Sir3 bound domains covered on average ~15 kb and up to ~22 kb upon 16 or 29 fold overexpression (Fig1D). Subtelomeric domains covered by Sir3 were undistinguishable (pearson correlation 0.98, p-val < 1.e-16) in 16x[Sir3] and 29x[Sir3] strains (Fig1F). Sir3 binding domains expansion upon increase of dosage thus reaches saturation for Sir3 levels superior to 9x and inferior to 16x. Supporting this interpretation, we observed that the level of nuclear background Sir3-GFP fluorescence is almost doubled in 29x strains compared to 16x strains (SupFigS1C).

Heterogeneous expansion of subtelomeric domains upon increase of Sir3 expression

Interestingly individual telomeres showed very different behaviours in response to Sir3 dosage elevation. We established four stereotypical categories (Fig1F):

Consistent with the average binding profiles, the largest group (12/26) is composed of subtelomeres at which Sir3 spreading increased progressively with Sir3 dosage, reaching saturation at 16X. Two other groups were distinguished on the basis of their response to the first increase in Sir3 levels. Sir3 binding directly reached its saturation state in a second group (6/26), whereas it only changed upon 16x increase at four subtelomeres (4/26). Lastly, 3 subtelomeres were apparently insensitive to Sir3 levels changes.

Irrespective of the different impact of changes in Sir3 concentration depending on the subtelomere, Sir3 occupancy at saturation covered diverse domain lengths (ranging from 7kb to 25kb -HM excluded-), independently of chromosomal arm length or middle repeats content. Sir3 spreading ends right before essential genes at three subtelomeres (*RPN12* at TELVIR, *ERO1* at TELXIIIL and *GAB1* at TELXIIR). Lastly, we found only few examples of euchromatic nucleation sites that were revealed upon Sir3 overexpression (SupFigS1E).

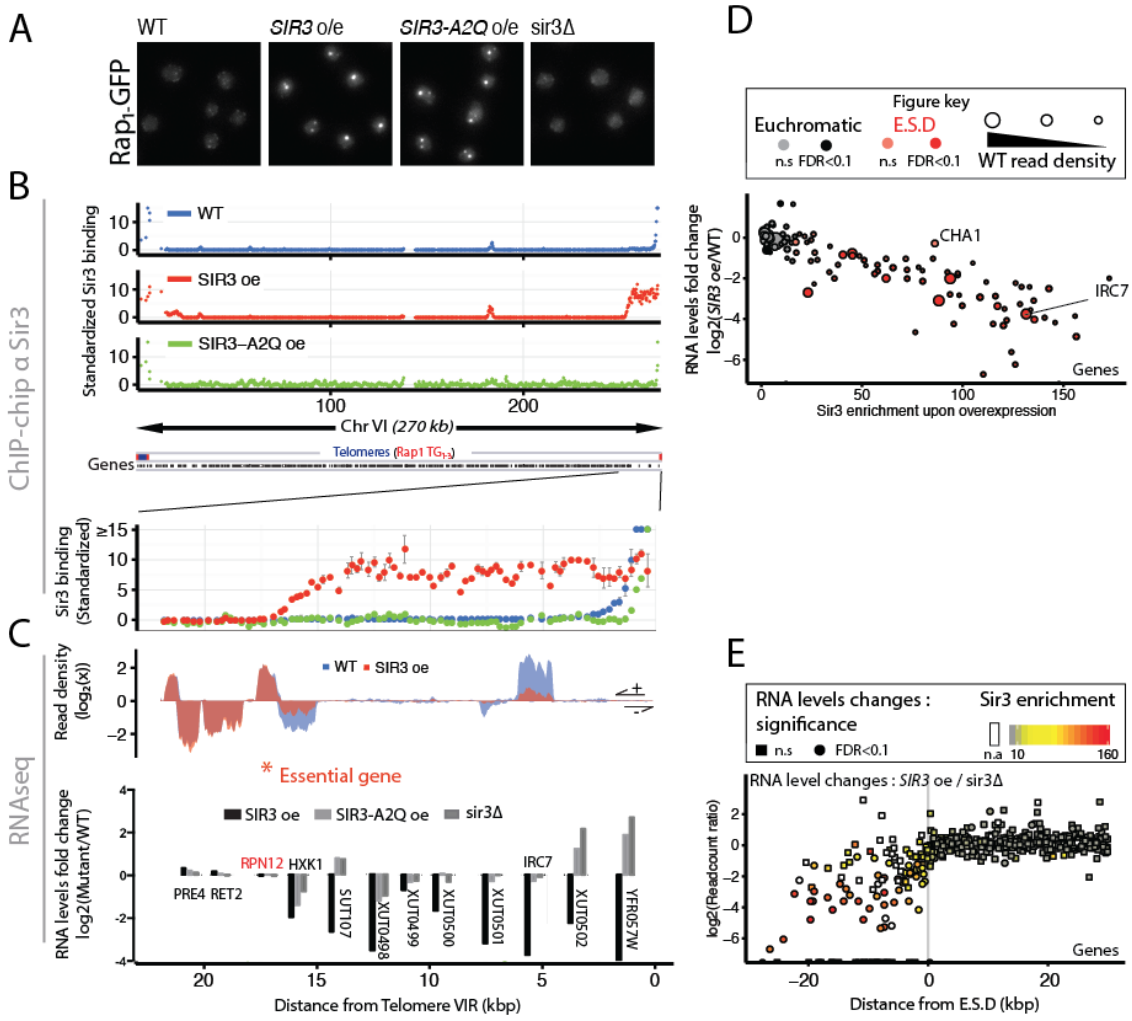

Figure 2 Sir3 extended domains are silenced and restricted to subtelomeres. (A) Representative Rap1-GFP images of exponentially growing strains differing for Sir3 amount or expressing the SIR3-A2Q point mutant. (B) Chromosome wide binding of Sir3 in the same strains as in A and blow-up on subtelomere VIR. Enrichment is measured as the standardized IP over Input and scale is thresholded at 15 for visualization purposes. (C) Total RNAseq read density and corresponding RNA level fold change along subtelomere VIR in indicated exponentially growing (OD~1) strains. (D) Sir3 binding and corresponding RNA level changes of subtelomeric genes (Distance from chromosome end <50 kb) upon overexpression of SIR3. Color code indicates if a gene is annotated as within E.S.D (see math et meth) and shade indicate significance (FDR<0.1) of the detected changes. Read density in WT cells is proportional the disk area. (E) RNA level changes in function the distance from the end of silent domains. Symbols indicate significance and color code indicate Sir3 enrichment averaged over gene bodies.

Thus, Sir3 propagation reaches saturation for different amount of Sir3 depending on which subtelomere is probed. Overexpression of *SIR3* creates continuous Sir bound domains of heterogeneous extents at individual telomeres.

Telomere hyperclustering has a minor impact on transcription

It was shown that increasing Sir3 levels extend subtelomeric silent domains by genetic assays (Renauld et al. 1993b; Strahl-Bolsinger et al. 1997; Ruault et al. 2011b) and telomere

clustering by microscopy (Ruault et al. 2011b). However, the direct impact of telomere clustering on transcription is unknown. To address this question, we took advantage of a strain overexpressing the Sir3-A2Q point mutation. This mutant is impaired for gene silencing yet competent for telomere clustering (X. Wang et al. 2004; Ruault et al. 2011b) (Fig2A). We probed Sir3-A2Q binding and confirmed that the binding of this mutant is restricted to nucleation sites (Fig2B). Next we conducted transcriptome analysis by RNAseq to compare p*GPD-sir3-A2Q* to p*GPD-SIR3* strains, to uncouple the effects mediated by Sir3 silencing function from the potential impact of telomere clustering.

The cells overexpressing Sir3-A2Q exhibited a transcriptional signature consistent with a partial loss of *HM* silencing, the amplitude of the pseudo-diploid transcriptional response being smaller than in sir3Δ (SupFigS2C). This last observation demonstrates that this mutant, when overexpressed can achieve partial silencing at the *HM* even if its spreading capacities are impaired. In agreement with the inability of Sir3-A2Q to spread on chromatin, we observed almost no difference in the steady state RNA levels of subtelomeric genes when we compared the *sir3Δ* strain to the *GPD-Sir3-A2Q strain* (SupFigS2E). We observed two exceptions, *HXK1* and *PHO89,* that were down-regulated upon Sir3-A2Q overexpression. The down regulation of *HXK1* (Fig2C) might reflect the fact that the perinuclear localization of this gene contributes to its optimal expression (Taddei et al. 2006). Perinuclear localization of *HXK1* is probably lost in a GPD-Sir3-A2Q strain since telomeres relocalize in the nuclear interior upon sir3A2Q overexpression (Ruault et al. 2011b). Thus globally neither telomere clustering nor internal localization of telomeres impact the basal transcriptional status of subtelomeric genes in strains overexpressing the *sir3-A2Q* allele.

Extended heterochromatin domains are functional for silencing

In contrast, overexpression of Sir3 strongly decreased subtelomeric genes RNA levels. The extension of Sir3-bound domains upon Sir3 overexpression systematically led to the repression of underlying transcripts, independently of their coding status as exemplified for the right subtelomere of chromosome VI (Fig2C) and genome-wide (Fig2D). At the 26 subtelomeres included in our study, extended silent domains (ESD) included 100 genes that were not bound by Sir3 in WT cells. Differential expression analysis indicated that transcripts affected by Sir3 binding were all repressed.

We observed that the logarithm of transcriptional repression was linearly proportional to Sir3 binding signal, reflecting the absence of escapers from silencing and the good agreement between RNA-seq and ChIP-chip results. Interestingly, repression was largely independent of initial transcript level (Fig2D). To gain access to the expression of repeated gene families we carried out a second analysis including reads mapping to multiple loci (see material and methods). It appears that entire gene families characteristic of subtelomeres and Y' elements are repressed upon Sir3 overexpression (SupFigS2B, S2F) suggesting that the portion of subtelomeres devoid of chip probes is collectively silenced.

RNA levels do not account for the extent of Sir3 spreading upon overexpression of *SIR3*

We next aimed to identify the mechanisms that could limit the extent of Sir3 spreading. To test directly whether the limit to Sir3 spreading is dependent on the distance covered by the SIRs, we compared Sir3 spreading at the wild type telomere VIIL versus a 15 kb truncated version. Strikingly, in both cases Sir3 binding ended within the *HXK2* promoter (Fig3F), with a somewhat sharper decline rate in the truncated strains. This comparison indicated that the determinants of Sir3 bound domain ends are either defined relative to the core of the chromosome or depend of local features.

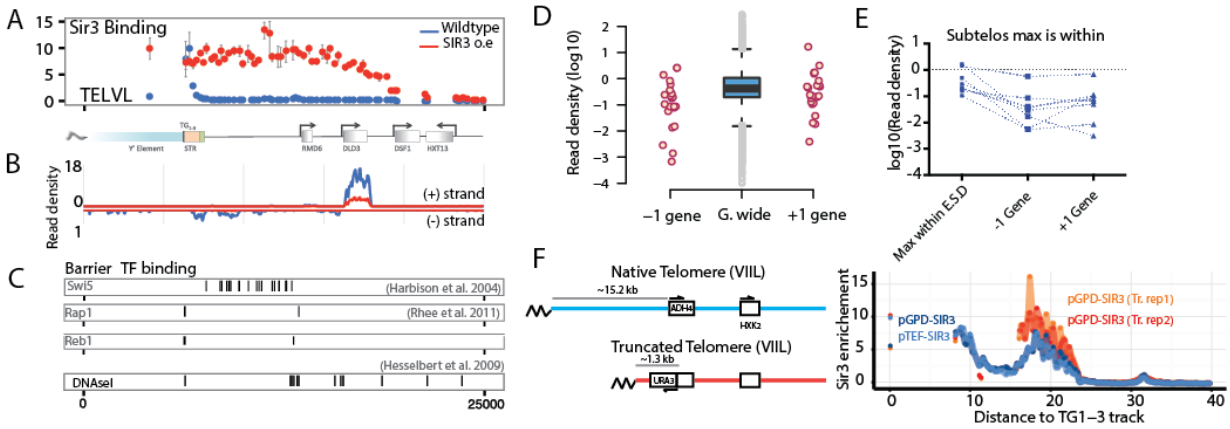

Figure 3 End of extended silent domains is defined locally and independently of transcriptional activity (A) Sir3 binding at TELVL in WT and Sir3 overexpressing (pGPD-SIR3) strains, X-axis coordinate is shared with B and C. (B) Corresponding read density along plus (upper curve) and minus (lower curve) strands. (C) Transcription factor binding and DNAseI hypersensitive sites along TELVL (D) Read density of genes located before and after the end of extended silent domains compared to genome wide distribution (central boxplot) (E) Same as F exemplifying the 7 subtelomeres at which a gene within E.S.D show larger transcript amount than the genes located at the end of the domain. (F) Sir3 binding at native and truncated TELVIIL, x coordinates correspond the native telomere VIIL

Focusing on silent domains ends, we quantified the slope of Sir3 binding profile in the strains overexpressing SIR3 at each subtelomere whenever it was possible (24/32 subtelomeres). We observed that the slope at the end of a silent domain is not correlated to the distance from the telomere (*i.e* nucleation point) and found no correlation with the groups defined based on the response to Sir3 dosage changes (SupFigS3A).

We conclude that when the dose of silencing factor is not limiting the spread of heterochromatin, the delineation of the silent domain does not depend on the distance from the nucleation site. Our results rather suggest that extended silent domains are defined relative to the core chromosome.

Most genes covered by Sir3 upon overexpression are lowly expressed in wild-type cells, which could argue that Sir3 spreading is limited by transcription. However, this not the case as we could find highly expressed genes lying within ESD as exemplified by IRC7 (Fig2A) and DLD3 (Fig3A). Both genes belong to the decile of most expressed genes (Fig3D) and to the first quartile of most frequently transcribed genes in wild-type cells (Pelechano, Chávez, and Pérez-Ortín 2010). Despite these high transcription rates, these two genes are repressed upon Sir3 binding, indicating that transcriptional activity per se is not sufficient to stop Sir3 spreading. Accordingly, at 7 subtelomeres at least one gene within the ESD had higher read density than the gene adjacent to the ESD (Fig3F). While the limitation of Sir3 spreading could be the consequence of the counter selection of cells silencing essential genes, we do not favour this hypothesis. It is noteworthy that no essential genes were found within ESD and that 3 ESDs ends are contiguous to three essential genes. However, we did not detect significant decrease in mRNA levels for these genes upon Sir3 overexpression suggesting that they are protected against Sir3 spreading.

Punctual binding sites of barrier factors are not efficient barriers to silencing

As mentioned above, we observed a 3-fold (2.96) repression of Y' elements upon Sir3 overexpression (SupFigS2F), which implies that the barrier effect mediated by Tbf1 and Reb1 (Fourel et al. 1999) does not hold, at least at a fraction of Y' containing telomeres or in a fraction of the population. To explore the possibility that other DNA sequence specific barrier elements are involved in the confinement of Sir3 within subtelomeres, we listed all the transcription factors that have been proposed to have a barrier activity, and

concatenated binding data when available, ending up studying the binding of 10 transcription factors (Adr1, Gcn4, Rgt1, Hsf1, Sfp1, Reb1, Abf1, Leu3, Swi5: Harbison et al. 2004, Rap1 : Rhee et al. 2011 ,Tbf1 Preti et al. 2010).

We identified DNA-sequence specific elements, reported to have barrier activity, in the first genes before or after the end of the E.S.D at 12 subtelomeres (SupFigS3); However, each of these factors were also found at other sites within the E.S.D (Fig3C) indicating that those factors alone are not sufficient to limit the propagation of the SIR complex.

We found known barrier elements flanking Sir3 bound domains at the three subtelomeres that were categorized as insensitive to Sir3 levels (group4). Silent domain invariably remains constrained by the Leucine tRNA at subtelomere IIL. A previously identified barrier sequence homologous to the left barrier of HML (Xin Bi 2002) lies at the end of subtelomere XIR Sir3 binding domain, while the right end of subtelIIIL silent domains is irresponsive to Sir3 dosage, likely as a consequence of the directional properties of the I silencer (Fig S3B).

Thus, with the exception of these three subtelomeres, we could not identify the factor blocking the extension of silent domains.

Sir2 activity is a minor limitant of SIR spreading

A possible limitation to silent chromatin spreading is the capacity of the SIR complex to deacetylate H4K16 residues. We reasoned that this might be particularly relevant when Sir3 is not limiting the propagation of the SIR complex.

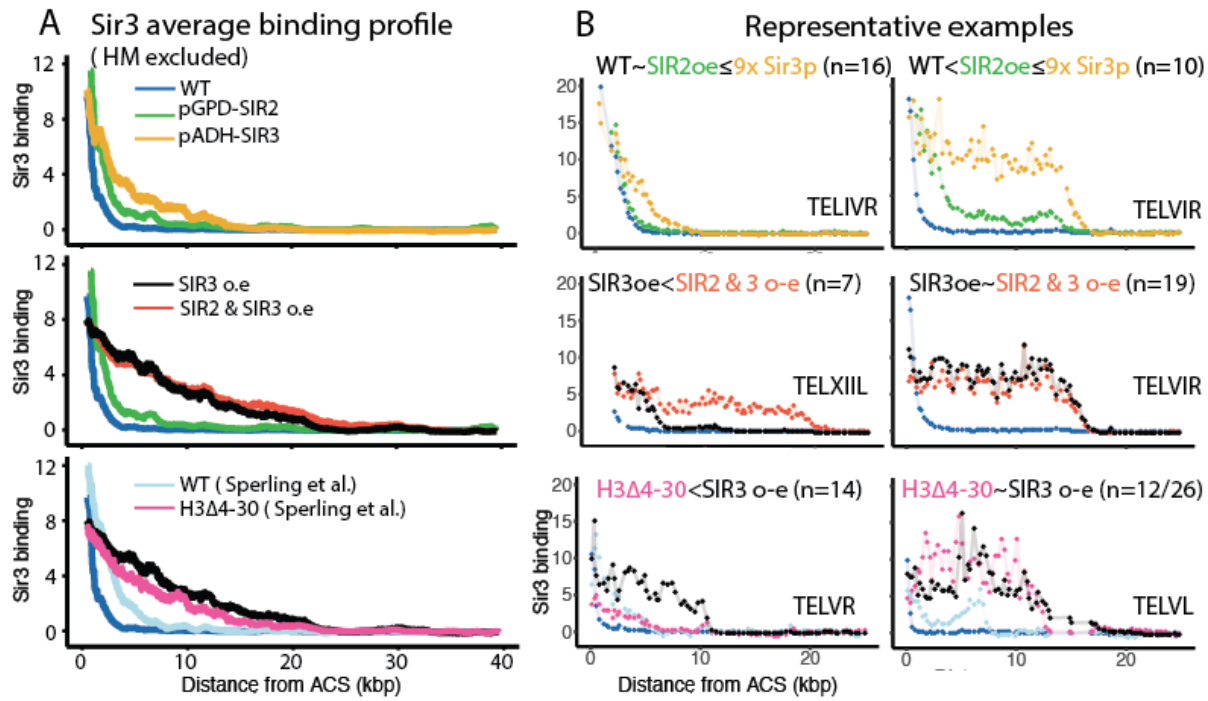

Figure 4 H3 & H4 acetylation is a major buffer of silent domain extension (A) Moving average of Sir3 binding at telomeres (with the exception of TELIIIL and TELIIIR which contain HM loci) as in fig1F, in the indicated genotypes. (B) Representative examples of Sir3 binding in the indicated genotypes. Qualitative comparison of Sir3 spreading between conditions is indicated as legend with the number of subtelomere attributed to this stereotypical category.

Consequently, we probed the effect of increasing Sir2 dosage on Sir3 spreading. We monitored the genome wide occupancy of Sir3 in strains overexpressing Sir2 and in strains co-overexpressing Sir2 and Sir3. On average Sir3 binding profile progresses toward centromeres upon Sir2 overexpression, but to lesser extend than upon 9x Sir3 overexpression (Fig4A). Sir3 bound domains extended at a subset of 12 subtelomeres, 11 of which were also extended upon mild -9x- Sir3 overexpression (11/12). However, at these subtelomeres Sir3 enrichments were lower upon Sir2 overexpression than upon Sir3 overexpression (Fig4B). We note that whereas the overexpression of Sir3 had no apparent effect on its propagation at the left border of the rDNA array, Sir3 binding was extended upon overexpression of Sir2. At this locus, a tRNA restricts the binding of the SIR or the RENT complex, and protects the essential acetyl-Coa synthetase gene *ACS2* from deleterious silencing (Biswas et al. 2009).

We next turned our attention to strains co-overexpressing Sir2 and Sir3. To our surprise, in most cases overexpression of Sir2 had no effect (20/26). Only in a minority of cases Sir3

spreading was increased in strain co-overexpressing Sir2 and Sir3 (Fig 4B). In the latter cases E.S.D remained devoid of essential and tRNA genes.

We conclude that at a majority of subtelomeres, Sir2 activity is not limiting the spread of heterochromatin even when sir3 is over-abundant. As Sir3 bound domains were either unchanged or extended upon Sir2 and Sir3 co-overexpression, we deduced that Sir3 and Sir4 were not limiting the extension of silent domains in the strain overexpressing Sir3. Collectively, this lent credence to the notion that we reached a situation in which spreading is likely limited by local chromosomal features, leading to the blocking of the extension phenomenon.

Sir3 overexpression mimics the absence of H3 tail acetylation at a subset of subtelomeres

Albeit the mechanistics are still obscure, several studies point to a role of H3 tail acetylation in limiting silencing (Thompson, Ling, and Grunstein 1994; Kristjuhan et al. 2003; Sperling and Grunstein 2009). In detail, Sir3 bound domains extend at half of subtelomeres in a mutant expressing a histone with truncated tail, H3Δ4-30. Consistent with a prominent role of acetylation in this process, mutation of the 5 acetylable lysines located on H3 tail (K9, 14, 18, 23 and 27) led to a similar extension of Sir3 bound domains (Sperling and Grunstein 2009). We undertook to compare the effect of Sir2/3 overexpression to the effect of disrupting H3 acetylation on Sir3 binding using published data (Sperling and Grunstein 2009) and to compare telomere clustering in those mutants.

First we noticed that the subtelomeres that were insensitive to Sir3 dosage were also insensitive to changes in H3 tail acetylation. Globally, we found that when effective, disruption of H3 tail acetylation had a greater effect on Sir3 spreading than Sir2 overexpression (Fig4A). Among the 18 subtelomeres at which Sir3 binding is extended in the H3Δ4-30 mutant, most had Sir3 binding profiles similar and in some cases identical to the one obtained at a given level of Sir3 overexpression: for example, 9x for the IL, 16x for the VL (Fig4B). However, contrary to strains overexpressing Sir3, telomere clustering was not affected in H3Δ4-30 mutants (SupFigS4).

Overall, those results demonstrate that Sir2 activity is a minor limitation of SIR complex propagation relative to H3 tail acetylation. Furthermore, comparing H3 tail mutants to strains overexpressing Sir3 led us to conclude that extension of Sir3p binding in subtelomeric regions is not sufficient to promote the clustering of telomeres. Lastly the similarities of Sir3 bound domains in H3 tails mutants and in strains overexpressing *SIR3* suggest that the domains defined by overexpression of Sir3 likely exist independently of Sir3 dosage.

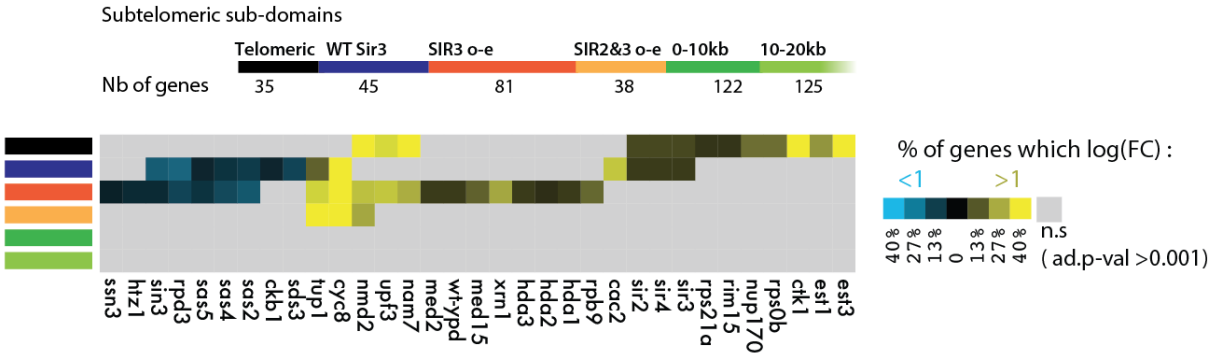

Figure 5 Localized effects of mutations affecting subtelomeric transcription. The different subtelomeric sub-domains are defined according to Sir3 binding (See material and methods), and the number of genes present in each domain and in (Kemmeren et al 2014) is indicated. Grey areas are zone in which no enrichment was detected. Color code indicate the proportion of genes which fold change is > 2.

Identification of subtelomeric sub-domains

Based on our description of the different Sir3 binding domains unveiled by Sir3 or Sir2 and Sir3 overexpression, we searched for factors having a localized effect within these subtelomeric subdomains. To this end, we analysed a compendium of over 700 transcription profiles (Kemmeren et al. 2014) for mutants having a significant impact on the subtelomeric domains previously defined. We classified subtelomeric genes into four different groups. The genes or pseudo-genes associated to middle repeat elements constitute the first group. The remaining three groups are the genes bound by the Sirs in WT cells, the genes to which Sir3 has access upon saturated overexpression and the genes to which Sir3 binds following co-overexpression of Sir2 and Sir3. To search for potential factors having a localized effect at the domains flanking the one we described, we also consider the group of genes located within 10kb from the end of Sir3 accessible subtelomeric domains (SASD) and located

between 10 and 20kb from SASD ends. For each mutant we tested if the proportion of genes up or downregulated (|log2(FC)|>2) within a given subtelomeric domain is higher than expected by chance, considering the effect of the mutation on the genome. The main outcome of this analysis is the identification of genes which mutation only affects particular subtelomeric subdomains (Fig5). With this approach, the transcriptional outcome of sir2, sir3 or sir4 deletion were as expected restricted to 'telomeric' and 'WT Sir3 bound domains. Twenty other mutants have a significant impact on the expression of these two domains, including mutants previously known to affect subtelomeric transcription such as telomerase components, the nucleoporin NUP170 (Van De Vosse et al. 2013), the mediator complex tails proteins Med2 and Gal11(Peng and Zhou 2012; Lenstra et al. 2011), the hda1/2/3 complex, components of the non-sense mediated mRNA decay pathway and the repressors Tup1/Cyc8. While the direct contribution of ribosomal proteins to telomere clustering has been reported, we found that rps0b and rps21 mutants specifically affect transcription of the telomeric domain. More importantly, we observed that gene silencing due to Sir spreading in rpd3 or sas2/4/5 mutants does not extent further than the domains observed upon overexpression of Sir3 implying that those genes are likely not responsible for the restriction of Sir3 upon overexpression. At last, no mutant had a significant localized effect outside of the domains defined by Sir3 overexpression. Even if the dataset chosen does not cover all gene deletions, this last observation indicate that subtelomeric position effects, in their broad acceptation, are likely absents outside of the domains defined.

A specific chromatin landscape pre-exist in Sir3 accessible domains

To seek for potential chromatin determinants of silent domain propagation and limitation, we analyzed the genome wide distribution of 26 histone marks or variants (Weiner2015). We first computed the correlation between Sir3 binding signal and histone modifications at subtelomeres. Consistent with previous results, we recovered the anti-correlation expected between Sir3 binding and H4K16 acetylation in wild type cells. Interestingly, we observed that upon overexpression, Sir3 binding signal is better correlated with histone H3 methylation and histone H2A phosphorylation (Fig6A &B). This implies that probing Sir3

binding upon overexpression somehow reveals the subtelomeric chromatin landscape of wild type cells.

Next, we probed histone marks distribution within the different ChIP-defined subdomains previously described. Sir bound nucleosomes were depleted of most histone marks, with the exception of H4R3 methylation and H2A phosphorylation, which were enriched within silent domains, as expected. A second category of marks were depleted from silent domains but enriched within the SASD and at background levels past SASD. Within SASD, the average nucleosome is hyper-acetylated at H3K27 and H4K5,8,12 and mono methylated at H3K79. In addition, we observed that the histone variant H2A.Z is enriched with SASD (Fig 6B, C & SupFigS6).

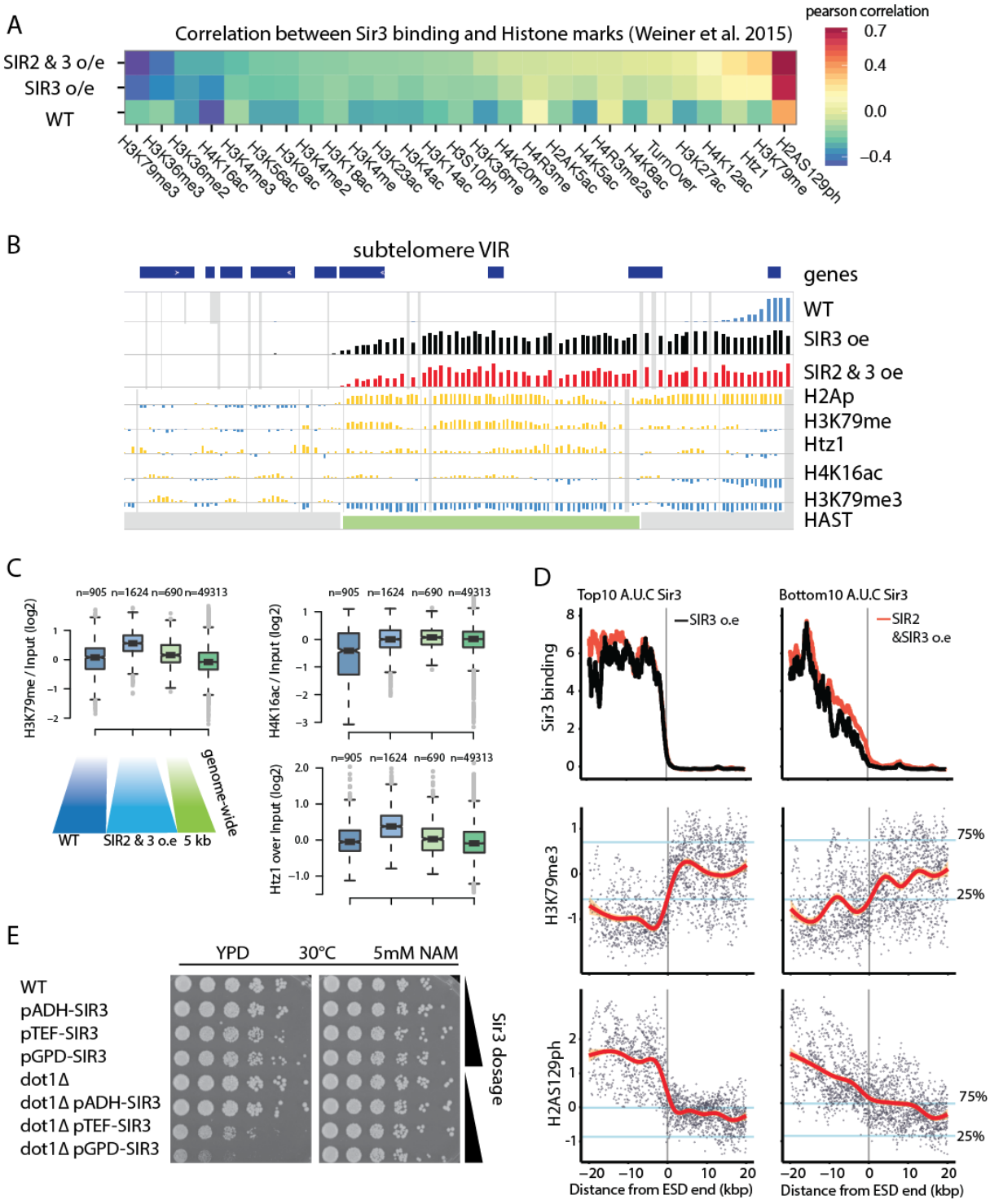

Figure 6 Subtelomeric chromatin landscape structuration correlates with silent domain expandability and shed light on the protective role of H3K79 methylation (A) Pearson correlation matrix between Sir3 binding and histone marks, SIR3 oe corresponds to yAT1254 and SIR2 & 3 to yAT1668. (B) Genome browser visualization of Sir3 binding in WT, pGPD-SIR3 or pGPD-SIR2 pGPD-SIR3 strains and selected histone modification or variants (from Weiner et al. 2015) in WT strains at TELVIR. Border of H.A.S.T domains were obtained from Robyr et al. 2002. (C) Distribution of selected histone marks relative to H3 (data from weiner et al.2015) along wild type silenced domains and within the contiguous subtelomeric domains accessible to Sir3 upon overexpression. As a control the distribution of those marks within the 5 kb contiguous to the end of extended silent domains as well as the genome wide

distribution of those marks is shown. (D) Moving average of Sir3 binding at telomeres. The top and bottom 10 telomere with regards to Sir3 signal in strains overexpressing Sir2 and Sir3 were plot separately. The two histone marks the best associated (either positively or negatively correlated) are shown in the same groups. Genome wide lower and higher quartiles for each mark are indicated by blue line. Red line correspond to the local smoothing of histone modification data (E) Dot assay to probe viability of dot1 mutants upon overexpression of Sir3. Cells were constantly grown in presence of 5mM Nam prior to this assay. Cells were grown overnight, and 0.5 O.D of cells were plated in 5x serial dilution on YPD or YPD 5mM NAM.

In contrast, we observed that the depletion of H3K4, H3K36 and H3K79 tri-methylation extends until SASD ends. A notable exception was H2A phosphorylation which enrichment is still significant within the 5kb flanking SASD ends. We reasoned that the longer intergenes present within subtelomeres might bias our analysis, artificially leading to the depletion of marks associated to gene bodies. To control for this potential artifact source, we conducted a second analysis, separating promoter nucleosomes (-3, -2, -1) from gene body nucleosomes and obtained essentially the same results (not-shown).

In a complementary approach, we focused on Sir3 binding domains ends. We classified each subtelomere according to the area under the curve (AUC) corresponding to the logistic-like fit of Sir3 binding signal upon co-overexpression of Sir2 andSir3 (See mat & meth). It appears that at the ten telomeres showing the highest AUC, several histone marks display sharp changes. This is especially true for H3K79me3, H3K36me3 and H2AS129P. In contrast, the bottom ten subtelomeres in terms of Sir3 AUC show rather smooth changes (Fig6D). Thus, upon overexpression Sir3 extends on a pre-existing chromatin landscape associated with specific histone modifications (low levels of H3K79me3 and H3K36me3 and high levels of H2AP).

H3K79 methylation is essential to protect euchromatin from the spread of silencing

Our results demonstrate that when extendable, the end of WT silent domains are generally located within a subtelomeric area devoid of H3K79me3 and enriched for H3K79me1. In contrast, SASD ends coincide with H3K79 tri-methylation discontinuity zone. As H3K79 methylation has been shown to impair Sir3 binding in vitro (Altaf et al. 2007; Wang 2013), this mark appeared as a good candidate to stop Sir3 spreading when overexpressed.

To test this hypothesis, we overexpressed Sir3 in this absence of Dot1, the only methyltransferase responsible for H3K79 methylation, we found that the *GPD-SIR3 dot1Δ* strains are extremely sick and are generating suppressors upon streaking. To avoid any artifact due to these potential escapers, we designed a transformation experiment in which the *dot1Δ* mutant is transformed with the *GPD-SIR3* construct in the presence of 5mM NAM that efficiently inhibits silencing. After selection of positive clones, we assessed the growth of those mutants on medium without NAM, allowing initiation of silencing in the presence of large excess of Sir3, similarly to what has been done in (Osborne, Dudoit, and Rine 2009). Our results showed that Dot1 is essential to sustain viability when Sir3 is overexpressed (Fig 6E). We used the same method to test the requirement of other histone modifiers in the context of increased Sir3 dosage. In contrast to Dot1, Set1 or Set2, which deposit H3K4 and H3K36 methylation, marks, or the histone de-acetylase Rpd3 were dispensable for viability in presence of high Sir3 dosage (SupFig6). Thus among the chromatin modification best anti-correlated with Sir3 binding, only H3K79 methylation appears essential to restrict the ectopic spread of silencing. Interestingly, the phenotype of *dot1* mutants overexpressing Sir3 was only appreciable at Sir3 amounts above 9x. In those cases, lethality of *dot1Δ SIR3* o/e was fully rescued by 5mM NAM treatment (Fig6E). Overexpression of the *Sir3-A2Q* point mutant in a *dot1Δ* strain was viable and leads to the hyperclustering of telomeres, demonstrating that the lethality of *dot1* mutants overexpressing *SIR3* is not due to the clustering of telomeres (SupFigS6). In addition, co-overexpression of *DOT1* and *SIR3* leads to loss of silencing, showing that H3K79 methylation prevails on Sir3 binding (Sup fig6C).

Intrigued by the observation that mono and tri-methylation state of H3K79 showed opposite behaviors, we hypothesized that the two methylation state might have different functions regarding silencing. *bre1* mutants are lacking H3K4me3, H3K79me3 methylation and have increased H3K79me1 (Frederiks et al. 2008). As set1 mutants overexpressing Sir3 were viable we reasoned that potential effect of bre1 deletion would likely come from H3K79 methylation changes. Interestingly, while *bre1* mutants over-expressing Sir3 29x have subtle growth defect when grown at 30°C, they do not sustain viability at 37°C. As for *dot1*, *bre1* lethality is rescued by 5mM NAM treatment, suggesting that the absence of H3K79me3 allows deleterious transcriptional silencing, with acute effects at 37°C. Our results are consistent with a distinct role of the different methylation of H3K79 in silencing restriction.

Discussion

The Sir complex has been a model for chromatin complex propagation and gene silencing for decades. Pioneer studies demonstrated that increasing the dose of Sir3 extends silenced domains at subtelomeres (Renauld et al. 1993b; Pryde and Louis 1999), a property common to several heterochromatin complexes. However there has been controversy on the generality of this finding at natural telomeres (Pryde and Louis 1999), and the details of this process along with its link with telomere clustering (Ruault et al. 2011b) remain unclear. Here we systematically studied the impact of increasing Sir2 and Sir3 dosage on the propagation of the SIR complex, on the clustering of telomeres and on genome wide transcription.

Gradual overexpression of Sir3 revealed that the increase in telomere clustering and the concomitant spreading of Sir3 over subtelomeres reaches saturation for Sir3 levels between 9 and 16x. Surprisingly the responses to increase in Sir3 levels were not continuous at all subtelomeres as Sir3 spreading was only affected above a certain threshold of concentration at some subtelomeres. At 29x Sir3, extended silent domains covered at least an additional 226 kb, associated with the repression of a hundred of genes. However, while most telomeres are clustered in those conditions, the spreading of Sir3 along subtelomeres varied greatly depending on the subtelomere probed. At few subtelomeres silent domains are already constrained by punctual elements in wild type cells while at others the extension observed varied up to 30 kb this extent being largely independent of middle repeat elements or chromosomal arm length.

Irrespective of the extent of the subtelomeric domain covered by Sir3 we observed that the relationship linking Sir3 binding to transcriptional repression is largely independent of the gene or subtelomere under consideration. This suggests that silencing efficiency is largely dictated by the ability of Sir3 to associate with chromatin. Accordingly, the domains covered by Sir3 upon overexpression shared similar chromatin marks suggesting that the chromatin landscape is the main determinant of maximal Sir3 spreading extension.

Our data indicate that the methylation of H3K79 by Dot1 is required for viability when Sir3 is present in large excess. Our work determines the maximal subtelomeric domains accessible to the Sir complex and uncovers previously uncharacterized descrete chromosomal domains. This approach is an original way of probing the extent of subtelomeric chromatin specificities.

Reaching the borders of subtelomeric silent domains

By overexpressing Sir3 at different levels, we studied the dose dependency of heterochromatin spreading at equilibrium. Our data are qualitatively different from previous genome wide studies that described Sir3 binding after 4 hours of induction (Radman-Livaja et al. 2011), out of equilibrium (Katan-Khaykovich and Struhl 2005). Co-overexpression of Sir2 and Sir3 demonstrated that Sir2 activity is not limiting Sir3 spreading at most subtelomeres. In addition, as few silent domains were extended in those conditions, we deduced that Sir4 was not limiting the extension of the subtelomeres unaffected by the additional overexpression of Sir2. As ESD were associated to different middle repeat elements and were of different length, we ruled out a potential effect of nucleation site, and a potential maximal size of silent domains that would be intrinsically regulated. Current model depicting the limitation of heterochromatin spreading oppose negotiable and fixed borders (Kimura and Horikoshi 2004). Interestingly, only fixed borders are expected to be independent of Silencing factor concentration. Thus our results collectively suggest that the saturation of silent domain expansion likely correspond to the reaching of fixed borders along subtelomeres.

Different categories of Sir chromatin antagonism

At subtelomeres the extent of spreading of the Sir complex results from the contributions of the nucleation element strength, of chromatin modifying enzymes and Sir concentration (Gartenberg and Smith 2016; Grunstein and Gasser 2013). Ultimately, those parameters influence the affinity of Sir3 for chromatin. While most studies characterized in detail the effect of abrogating one or several chromatin modifying enzymes we chose to tune Sir3

concentration. At high concentrations of silencing factors we observed that Sir3 binding extends within regions that not only contain chromatin marks reported as antagonistic to its spreading but are even enriched for some of them such as the histone variant H2A.Z (Guillemette et al. 2005) and the mono-methylation of H3K79 (Altaf et al. 2007). Although this suggests the existence of fixed borders, our search for punctual border elements only retrieved convincing candidates at the three subtelomeres for which the extension was already limited in wild-type cells. Oppositely, we report that native binding sites occupied by transcription factors that block silencing when tethered to chromatin (Oki et al. 2004) are not efficient barriers to Sir3 spreading. This is perhaps not surprising for two reasons: first, there are precedent showing that multiple binding sites are required for efficient barrier effect (X Bi, Yu, Sandmeier, and Zou 2004). Second, the binding strength of those transcription factors is likely different than the one of the GBD used to target candidate barrier factors (Oki et al. 2004). Consequently, our work indicates that histone tail acetylation; H2A.Z presence and binding of some transcription factors are likely buffering the spread of the SIR rather than blocking it.

End of extended silent domains: the specific role of Dot1

We observed that the end of extended silent domains coincide with a major histone mark transition zone, characterized by the abrupt enrichment of H3K4me3, H3K36me3 and H3K79me3. While deletion of *SET1* or *SET2,* the genes encoding for the enzymes responsible for the two first marks had no impact on cell growth upon Sir3 overexpression, deletion of *DOT1* that encodes for the H3K79 methyltransferase was lethal in this condition.

Dot1 is a conserved enzyme, which enzymatic activity is distributive and leads to the mono, di or tri methylation of the lysine 79 of histone H3 (Stulemeijer et al. 2015). *In vitro,* binding of Sir3 to H3 peptides is abolished by mono, di and tri methylation of H3K79 (Altaf et al. 2007; Wang 2013). Using reconstituted nucleosomes, mono and di methylation reduces Sir3 affinity for nucleosome by a factor 5 for the tri methylation of H3K79 (Behrouzi et al, 2016; Martino et al, 2009). Studies of the crystal structure of Sir3-BAH domain bound to a nucleosomes predicts that methyl group contributes to decrease Sir3 affinity to nucleosome by decreasing the potential of K79 to form hydrogen bound with the BAH of Sir3 (Armache

et al. 2011). In contrast, in vivo study suggest that all levels of H3K79me states are functionally equivalent (Frederiks et al. 2008).

Nevertheless they exhibit differences in distribution and localization. Di-methylation is present at gene promoters and over gene bodies and H3K79 tri-methylation is restricted to gene bodies. The two methylation states differ in at least two major ways. First the di methylation is cell cycle dependent whereas the tri methylation is not (Schulze et al. 2009), second, only tri-methylation of H3K79 requires that nucleosomes carry the H2BK123Ub modification (Nakanishi et al. 2009; Schulze et al. 2009). At last, tri-methylation of H3K79 is not correlated to transcription frequency and its removal only occurs through histone turnover (Schulze et al. 2009; Weiner et al. 2015). Upon overexpression, Sir3 spreads over domains enriched for H3K79me implying that in vivo, this mark is not an obstacle to Sir3 spreading, which is in agreement with the observation that Sir3 is bound to H3K79me histones at telomeres (T Kitada et al. 2012). H3K79 di-methylation being mutually exclusive with tri methylation (Schulze et al. 2009), we hypothesized that loss of tri-methylation is responsible for allowing deadly spreading of the Sir. We reasoned that if H3K79me3 specifically blocks Sir3 spreading, then a bre1 mutant would have a similar phenotype as it is largely devoid of this modification (Nakanishi et al. 2009). However this is not exactly the case as this mutant is slow growing at 30°C yet non viable at 37°C. One interpretation of this observation is that the increased levels of H3K79me in bre1 mutants (Frederiks et al. 2008) are sufficient to slow down silencing spreading at 30°C, but fail to prevent ectopic spread of silencing at 37°C, a condition known to strengthen silencing (X Bi, Yu, Sandmeier, and Elizondo 2004). Our data thus indicate that the tri methylation of H3K79 observed at the boundary of extended silent domains block the spreading of Sir3 and thus protects euchromatin from heterochromatin.

Conversely co-overexpression of *DOT1* and *SIR3* led to loss of silencing. We propose that H3K79me3 mark has a specific function in the restriction of silencing, to which its cell-cycle independent status might contribute (Schulze et al. 2009). At last, we stress the observation that lethality associated to *SIR3* overexpression in *dot1* mutants is dose dependent. While we could not differentiate 16 and 29x Sir3 overexpression strains, they exhibited clear differences in the absence of Dot1 suggesting that the saturation of the dose-dependent increase in silencing is associated to Dot1 activity. We consider that the dose-dependency of

this process explains the apparent contradiction of our study with the results presented in (Verzijlbergen et al. 2009) and further exemplify the importance of probing different levels of overexpression.

Subtelomeric specificities

In most organisms, the specificities associated to chromosome ends extend beyond telomeres, within domains generally referred to as subtelomeres (Louis and Becker 2014). In budding yeast, several points of view enable to discern such specificities. Recent study comparing the conservation of synteny among closely related yeast species enabled a precise definition of budding yeast subtelomeres (Yue et al. 2017). It turns out that chromatin also exhibit specificities within domains located proximal to chromosome ends.

The first is undoubtedly the presence of heterochromatin, which has a unique signature in terms of histone marks. However specific properties associated to chromosome ends often extend beyond heterochromatic domains (Matsuda et al. 2015; Millar and Grunstein 2006). At most *S.cerevisae* subtelomeres, Hda1 affected subtelomeric (HAST) domains (Robyr et al. 2002) and Htz1 activated (HZAD) domains (Guillemette et al. 2005) lie contiguous to SIR silenced chromatin. In addition, phosphorylation of H2AS129 and mono methylation of H3K79 also extend further away than SIR silenced domains. When we compared the domain accessible to heterochromatin to HAST domains we observed that extended silent domains ends often coincide with a HAST domain end. Importantly, our study indicates that the subtelomeric domains revealed upon overexpression of Sir3 likely exist independently of Sir complex dosage, as other genetic contexts such as H3 tail mutants or tup1/ssn6 mutants also revealed similar regional effects. Interestingly, extension of silent domains reveals subtelomeric domains that possess consistent chromatin signature and define slightly different subtelomeres than synteny does. Accordingly we observed that the syntenic chromosome core is accessible to the SIR complex at 12 subtelomeres (SupFigS5). We recently showed that chromatin state impact on repair efficiency and outcome (Batté et al. 2017). This raises the question of whether the specific chromatin associated with subtelomeric domains that we uncovered in this study, contributes to the particular evolution of those regions.

Contribution of telomere proximity to subtelomeric properties

A central question of the biology of subtelomeres is to which extent the properties of subtelomeres are due to their proximity to telomeres or mere consequence of their gene content. Several studies demonstrated that the SIR complex contributes to the localization of enzymes to subtelomeres. For example, subtelomeric localization of the Okazaky fragment processing protein Dna2 is severely reduced in sir mutants (Choe et al. 2002). In addition, the kinase Tel1 responsible for H2A phosphorylation in subtelomeric regions is present at telomeres but H2AP levels depend mainly on the integrity of the SIR complex (Tasuku Kitada et al. 2011). Interestingly Sir3 stabilizes this mark even at regions where Sir3 is not detectable by ChIP in wild-type cells, suggesting that either Sir3 act remotely, or is binding these regions at least transiently in wild-type. Intriguingly, regions enriched for H2AP coincide with ESD leading to the hypothesis that overexpressing Sir3 stabilizes these transient interactions. Accordingly, profiling of Sir3 binding in G1 arrested cells demonstrated extended Sir3 binding domains at a subset of subtelomeres (Mitsumori et al. 2016) and Dam-ID profiling of Sir3 binding in set1/htz1 double mutants uncovered binding of Sir3 that were unnoticeable by ChIP (Venkatasubrahmanyam et al. 2007).

Conclusion

By taking the opposite approach to knock down of knock out studies, our work describes the dose dependency of budding yeast heterochromatin. In the presence of a large excess of silencing factors, ectopic nucleation of heterochromatin remains limited and does not impact euchromatic transcription. In contrast we observed the extension of subtelomeric silent domains and characterized their maximal extension along with the antagonistic factors that have been overcome, such as H2Az or H3K79me. The use of chromatin binding protein to scan chromatin properties enabled to uncover major subtelomeric histone mark transition zones, which functionally protects euchromatin from the spread of silencing. The long-term contribution of heterochromatin to the peculiar properties of subtelomeres will require further study.

Material and methods:

Media and Growth conditions: Yeast cells were grown on YP with 2% glucose, raffinose or galactose. All the strains used in this study were grown at 30 °C with shaking at 250rpm.

Yeast transformation protocol

Cells were seeded on liquid medium and grown to 0,8<OD_{600}<1,2. 3 ODs (~$3x10^7$ yeast cells) of cells were taken and washed with 1X TEL (10mM EDTA pH 8, 100mM Tris pH8, 1M Lithium Acetate), then 3µl of SSDNA (Sigma ref: D9156-5ML), DNA template (0,5µl if plasmid DNA, 5µl of digested plasmid or PCR product), 300µl of 1X TEL and 45% PEG-4000 solution were added. The mix was put 30 min at 30 °C and heat shocked at 42°c for 15 minutes. Lastly, cells were plated on appropriate selective medium.

Drop Assays

Yeast cells were transformed using the convential protocol expect that plating was made on selection plates supplemented with 5mM NAM. Pre-cultures were also made in YPD 5mM NAM. 5X serial dilutions are shown. Plates were grown for 2-3 days at the indicated temperature. When temperature is not shown it is 30°C.

RNA extraction and reverse transcription

RNA extraction was carried following RNeasy Mini kit instructions with DNAse treatment and using glass beads acid-washed for the mechanistic lysis. Total RNA integrity was assessed using nanodrop. 250ng or 500ng of total RNA was used as a substrate for reverse transcription by Super Script III enzyme using poly-A primers. Each experiment was made of 2-5 biological replicates.

Pellet preparation for ChIP

A total of 20 O.D equivalent of exponentially growing cells were fixed in 20 mL with 0.9 % formaldehyde for 15 min at 30°C, quenched with 0.125 M glycine and washed twice in cold TBS 1x pH 7.6. Pellets were suspended in 1mL TBS 1X, centrifuged and frozen in liquid nitrogen for -80°C storage.

Chromatin immunoprecipitation

All following steps were done at 4°C unless indicated. Pellets were re-suspended in 500 µL of lysis buffer (0.01% SDS, 1.1% TritonX-100, 1.2 mM EDTA pH 8, 16.7 mM Tris pH8, 167 mM NaCl, 0.5 % BSA, 0.02 $g.L^{-1}$ tRNA and 2.5 µL of protease inhibitor from SIGMA P1860) and mechanically lysed by three cycles of 30 s with 500 µm zirconium/silica beads (Biospec Products) using a Fastprep instrument (MP Biomedicals). Each bead beating cycle was followed by 5 min incubation on ice. The chromatin was fragmented to a mean size of 500 bp by sonication in the Bioruptor XL (Diagenode) for 14 min at high power with 30 s on / 30 s off and centrifuged 5 min at 13 000 rpm. 10 µL were kept to be used as Input DNA. Cleared lysate was incubated overnight with 1 µL of polyclonal antibody anti-Sir3 (Agro-bio). 50 µL of magnetic beads protein A (NEB) were added to the mixture and incubated for 4h at 4°C. Magnetic beads were washed sequentially with lysis buffer, twice with RIPA buffer (0.1% SDS, 10mM Tris pH7.6, 1mM EDTA pH8, 0,1% sodium deoxycholate and 1% TritonX-100), twice with RIPA buffer supplemented with 300 mM NaCl, twice in LiCl buffer (250 mM LiCl, 0.5% NP40, 0.5 % sodium deoxycholate), with TE 0.2% TritonX-100 and with TE. Input were diluted 10x with elution buffer (50mM Tris, 10mM EDTA pH8, 1%SDS) and beads were re-suspended in 100 µL elution buffer. A reversal cross-linking was performed by heating samples overnight at 65°C. Proteins were digested with proteinase K in presence of glycogen and the remaining DNA was purified on QIAquick PCR purification columns. Finally, samples were treated with 29 $\mu g.mL^{-1}$ RNAse A 30 min at 37°C.

ChIP-qPCR

1.2 µL out of the 50 µL of eluate and 2.4 out of 50 were used for qPCR reactions for the IP and the Input fractions respectively. qPCR reactions and analysis were done as in (Ruault et al., 2011). Values were either normalized by the enrichment at the OGG1 locus or at 0.2 kb from TELVIR. Error bars correspond to the standard deviation.

ChIP-chip preparation and hybridation

Samples used for ChIP-chip have all been analysed by qPCR prior to microarray hybridization. For microarray hybridization 4/5 of the immunoprecipitated DNA and of the DNA from the input were ethanol precipitated and re-suspended in 10µL of water (Gibco). Purified

material was amplified, incorporating amino-allyl-dUTP using as described in (Guidi et al. 2015). The size of amplified fragments (~500 bp) was assessed by gel electrophoresis. For each sample 1.5 µg of amplified DNA was coupled either with Cy5 (immunoprecipitated sample) or Cy3 (input sample) and hybridized on 44k yeast whole genome tiling array (Agilent) as described in (Guidi et al. 2015)

Microarray data acquisition, analysis and visualization

Microarray was imaged using a Agilent DNA microarray scanner and quantified using GenePix Pro6.1 as described in (Guidi et al. 2015).

Data analysis

All dataset were lifted over to Saccer3 when required. Histone marks data were obtained from (Weiner et al. 2015). Sir3 binding in H3 tail mutants from (Sperling and Grunstein 2009), nucleosome turnover from (Dion et al. 2007). Transcriptome data were downloaded from the website supporting the publication (Kemmeren et al. 2014). Subtelomere definition was obtained from (Yue et al. 2017). Zscores were computed using the R scale function.

Downsampling of Sperling data for figure 4 was done using R, visual inspection of the data confirmed that downsampling occurred without error. Average telomeric profiles were done by computing the mean of the signal over 10 kb windows separated by 10 bp.

The limits of Extended silent domains were computed as the first probes possessing 5 neighboring probes that have Zscore inferior to 1, starting from the telomere.

Fitting of the data was done using Matlab fitting toolbox using Bisquare robustess option. The function used is f(x)=K/(1+exp(-r*(-x+t0)))+1, with the following ftting parameters for K,r, and t0 : lower bounds : [10 0.0001 1000], Starting point : [10 0.0001 1000], upper bounds: [200 0.01 40000].

Area under the curve was exactly computed on the fitted signal of Sir3 binding in strains overexpressing *SIR2* and *SIR3*, 10kb before the end of silent domains and 5 kb after.

Mutants showing localized effects were identified with using the hypergeometric distribution, R function phyper with bonferroni correction for multiple testing (n=703).

Rap1 foci analysis:

The image analysis is performed with a slightly modified version of the dedicated tool from (Guidi et al. 2015). These modifications regard the quantification of foci and aim at providing a more accurate estimation of the quantity of fluorescence held inside each focus. The gaussian fitting approach has been replaced by a template matching framework with a bank of 100 symmetric 2D gaussian kernels with standard deviations ranging from 0.5 to 7 pixels. The position of each template is determined as the maximum of normalized cross correlation whereas the most suitable template for a single focus is selected by minimizing the sum of square differences between the gaussian template and the data within a circular mask of radius twice the standard deviation. The foci are then defined as spherical objects with radii of two times the standard deviations of the matched templates. All foci that could not be fitted were considered as a cube of dimension 5*5*5. Variation of the box size did not affect overall results. The foci intensity can thus be measured as the sum of the fluorescence signal inside its sphere. Furthermore, the proportion of intensity from a nucleus held inside each of its foci is also computed.

RNAseq

Total RNA from a 25mL culture of exponentially growing yeasts were extracted using phenol-chloroform. Libraries were constructed using the kit SOLiD Total RNA-Seq, with minor modifications : RNA are Zinc fragmented and fragments with size ranging form 100 to 200 nt selected by gel purification. After reverse transcription only fragment of size > 150nt are kept. Paired end (50 + 35) sequencing was done by the Institut Curie plateform. Differential expression was called using EdgeR, with a false discovery rate inferior to 0.1.

Author contributions :

A.H carried ChIP experiments, ChIP-chip hybridization and all the data analysis except RNA-seq read mapping (M.D) and upgrade of qFoci software (M.G). M.D designed the primary RNAseq analysis. M.R imaged most Rap1-GFP images. A.H. and M.R generated yeast strains. A.M co-designed the transcriptome experiment and participated in the elaboration of the project. A.H. and A.T. drafted the figures. A.H, A.T and M.R designed and interpreted experiments, and wrote the manuscript.

Acknowledgments :

We thank T. Rio Frio, S. Baulande and P. Legoix-Né (NGS platform, Institut Curie), A. Lermine (bioinformatics platform, Institut Curie), P.Lebaccon (PICT@Pasteur microscopy platform) for support. We also thank Camille Gautier for help with multiple mapping reads analysis and Marta Kwapisz for RNAseq library preparation. We thank Valérie Borde for help with microarray experiments, David Sitbon, Valérie Borde and Arnaud De Muyt for fruitful discussions, David Sitbon and Ann Ehrenhofer-Murray for critical reading of the manuscript. This work has benefited from the facilities and expertise of the NGS platform of Institut Curie (supported by the Agence Nationale de la Recherche [ANR-10-EQPX-03, ANR10-INBS-09-08] and the Canceropôle Ile-de-France), and of the high-throughput sequencing platform of IMAGIF (http://www.i2bc.paris-saclay.fr). A. Morillon's lab is supported by the Agence Nationale de la Recherche (DNAlife) and the European Research Council (EpincRNA starting grant, DARK consolidator grant). This work was supported by funding from the Labex DEEP (ANR-11-LABX-0044_DEEP and ANR-10-IDEX-0001-02 PSL) and from the ANR DNA-Life (ANR-15-CE12-0007). AH was supported by fellowships from the ENS PhD program and the FRM (DEP20131128535).

Bibliography :

Altaf, M, R T Utley, N Lacoste, S Tan, S D Briggs, and J Cote. 2007. "Interplay of Chromatin Modifiers on a Short Basic Patch of Histone H4 Tail Defines the Boundary of Telomeric Heterochromatin." *Mol Cell* 28 (6): 1002–14. doi:S1097-2765(07)00827-1 [pii]10.1016/j.molcel.2007.12.002.

Andrulis, E D, A M Neiman, D C Zappulla, and R Sternglanz. 1998. "Perinuclear Localization of Chromatin Facilitates Transcriptional Silencing." *Nature* 394 (6693): 592–95. doi:10.1038/29100.

Aparicio, Oscar M., Barbara L. Billington, and Daniel E. Gottschling. 1991. "Modifiers of Position Effect Are Shared between Telomeric and Silent Mating-Type Loci in S. Cerevisiae." *Cell* 66 (6): 1279–87. doi:10.1016/0092-8674(91)90049-5.

Armache, K.-J., J. D. Garlick, D. Canzio, G. J. Narlikar, and R. E. Kingston. 2011. "Structural Basis of Silencing: Sir3 BAH Domain in Complex with a Nucleosome at 3.0 A Resolution." *Science* 334 (6058): 977–82. doi:10.1126/science.1210915.

Batté, Amandine, Clémentine Brocas, Hélène Bordelet, Antoine Hocher, Myriam Ruault, Adouda Adjiri, Angela Taddei, and Karine Dubrana. 2017. "Recombination at Subtelomeres Is Regulated by Physical Distance,

Double-strand Break Resection and Chromatin Status." *The EMBO Journal*, e201796631. doi:10.15252/embj.201796631.

Bi, X, M Braunstein, G J Shei, and J R Broach. 1999. "The Yeast HML I Silencer Defines a Heterochromatin Domain Boundary by Directional Establishment of Silencing." *Proc Natl Acad Sci U S A* 96 (21): 11934–39. http://www.ncbi.nlm.nih.gov/pubmed/10518554.

Bi, X, Q Yu, J J Sandmeier, and S Elizondo. 2004. "Regulation of Transcriptional Silencing in Yeast by Growth Temperature." *J Mol Biol* 344 (4): 893–905. doi:S0022-2836(04)01270-7 [pii]10.1016/j.jmb.2004.10.002.

Bi, X, Q Yu, J J Sandmeier, and Y Zou. 2004. "Formation of Boundaries of Transcriptionally Silent Chromatin by Nucleosome-Excluding Structures." *Mol Cell Biol* 24 (5): 2118–31. http://www.ncbi.nlm.nih.gov/pubmed/14966290.

Bi, Xin. 2002. "Domains of Gene Silencing near the Left End of Chromosome III in Saccharomyces Cerevisiae." *Genetics* 160 (4): 1401–7.

Biswas, Moumita, Nazif Maqani, Ragini Rai, Srikala P Kumaran, Kavitha R Iyer, Erdem Sendinc, Jeffrey S Smith, and Shikha Laloraya. 2009. "Limiting the Extent of the RDN1 Heterochromatin Domain by a Silencing Barrier and Sir2 Protein Levels in Saccharomyces Cerevisiae." *Molecular and Cellular Biology* 29 (10): 2889–98. doi:10.1128/MCB.00728-08.

Choe, W, M Budd, O Imamura, L Hoopes, and J L Campbell. 2002. "Dynamic Localization of an Okazaki Fragment Processing Protein Suggests a Novel Role in Telomere Replication." *Mol Cell Biol* 22 (12): 4202–17. http://www.ncbi.nlm.nih.gov/entrez/query.fcgi?cmd=Retrieve&db=PubMed&dopt=Citation&list_uids=12024033.

Dion, Michael F, Tommy Kaplan, Minkyu Kim, Stephen Buratowski, Nir Friedman, and Oliver J Rando. 2007. "Dynamics of Replication-Independent Histone Turnover in Budding Yeast." *Science (New York, N.Y.)* 315 (5817): 1405–8. doi:10.1126/science.1134053.

Donze, D., and R. T. Kamakaka. 2001. "RNA Polymerase III and RNA Polymerase II Promoter Complexes Are Heterochromatin Barriers in Saccharomyces Cerevisiae." *EMBO Journal* 20 (3): 520–31. doi:10.1093/emboj/20.3.520.

Donze, David, Christopher R. Adams, Jasper Rine, and Rohinton T. Kamakaka. 1999. "The Boundaries of the Silenced HMR Domain in Saccharomyces Cerevisiae." *Genes and Development* 13 (6): 698–708. doi:10.1101/gad.13.6.698.

Donze, David, and Rohinton T. Kamakaka. 2002. "Braking the Silence: How Heterochromatic Gene Repression Is Stopped in Its Tracks." *BioEssays*. doi:10.1002/bies.10072.

Emil, Heitz. 1928. “Das Heterochromatin Der Moose.” *Jahrbücher Für Wissenschaftliche Botanik* 69: 762–818.

Fourel, G, E Revardel, C E Koering, and E Gilson. 1999. “Cohabitation of Insulators and Silencing Elements in Yeast Subtelomeric Regions.” *EMBO J* 18 (9): 2522–37. doi:10.1093/emboj/18.9.2522.

Frederiks, Floor, Manuel Tzouros, Gideon Oudgenoeg, Tibor van Welsem, Maarten Fornerod, Jeroen Krijgsveld, and Fred van Leeuwen. 2008. “Nonprocessive Methylation by Dot1 Leads to Functional Redundancy of Histone H3K79 Methylation States.” *Nature Structural & Molecular Biology* 15 (6): 550–57. doi:10.1038/nsmb.1432.

Gartenberg, Marc R., and Jeffrey S. Smith. 2016. “The Nuts and Bolts of Transcriptionally Silent Chromatin in Saccharomyces Cerevisiae.” *Genetics* 203 (4): 1563–99. doi:10.1534/genetics.112.145243.

Gotta, M, T Laroche, A Formenton, L Maillet, H Scherthan, and S M Gasser. 1996. “The Clustering of Telomeres and Colocalization with Rap1, Sir3, and Sir4 Proteins in Wild-Type Saccharomyces Cerevisiae.” *J Cell Biol* 134 (6): 1349–63.

Grewal, Shiv I S, and Songtao Jia. 2007. “Heterochromatin Revisited.” *Nature Reviews. Genetics* 8 (1): 35–46. doi:10.1038/nrg2008.

Grunstein, M. 1997. “Molecular Model for Telomeric Heterochromatin in Yeast.” *Curr Opin Cell Biol* 9 (3): 383–87. doi:S0955-0674(97)80011-7 [pii].

Grunstein, M, and S M Gasser. 2013. “Epigenetics in Saccharomyces Cerevisiae.” *Cold Spring Harb Perspect Biol* 5 (7). doi:10.1101/cshperspect.a017491.

Guidi, Micol, Myriam Ruault, Martial Marbouty, Isabelle Loïodice, Axel Cournac, Cyrille Billaudeau, Antoine Hocher, Julien Mozziconacci, Romain Koszul, and Angela Taddei. 2015. “Spatial Reorganization of Telomeres in Long-Lived Quiescent Cells.” *Genome Biology*. doi:10.1186/s13059-015-0766-2.

Guillemette, Benoît, Alain R. Bataille, Nicolas Gévry, Maryse Adam, Mathieu Blanchette, François Robert, and Luc Gaudreau. 2005. “Variant Histone H2A.z Is Globally Localized to the Promoters of Inactive Yeast Genes and Regulates Nucleosome Positioning.” *PLoS Biology* 3 (12): 1–11. doi:10.1371/journal.pbio.0030384.

Hoppe, G J, J C Tanny, A D Rudner, S A Gerber, S Danaie, S P Gygi, and D Moazed. 2002. “Steps in Assembly of Silent Chromatin in Yeast: Sir3-Independent Binding of a Sir2/Sir4 Complex to Silencers and Role for Sir2-Dependent Deacetylation.” *Mol Cell Biol* 12 (22): 4167–80.

Hoze, N, M Ruault, C Amoruso, A Taddei, and D Holcman. 2013. “Spatial Telomere Organization and Clustering in Yeast Saccharomyces Cerevisiae Nucleus Is Generated by a Random Dynamics of Aggregation-Dissociation.” *Mol Biol Cell* 24 (11): 1791–1800, S1–10. doi:10.1091/mbc.E13-01-0031.

Janke, C, M M Magiera, N Rathfelder, C Taxis, S Reber, H Maekawa, A Moreno-Borchart, et al. 2004. “A

Versatile Toolbox for PCR-Based Tagging of Yeast Genes: New Fluorescent Proteins, More Markers and Promoter Substitution Cassettes." *Yeast* 21 (11): 947–62. doi:10.1002/yea.1142.

Jia, Songtao, Ken-ichi Noma, and Shiv I S Grewal. 2004. "RNAi-Independent Heterochromatin Nucleation by the Stress-Activated ATF/CREB Family Proteins." *Science (New York, N.Y.)* 304 (5679): 1971–76. doi:10.1126/science.1099035.

Katan-Khaykovich, Y, and K Struhl. 2005. "Heterochromatin Formation Involves Changes in Histone Modifications over Multiple Cell Generations." *EMBO J* 24 (12): 2138–49.

Kemmeren, Patrick, Katrin Sameith, Loes A L Van De Pasch, Joris J. Benschop, Tineke L. Lenstra, Thanasis Margaritis, Eoghan O'Duibhir, et al. 2014. "Large-Scale Genetic Perturbations Reveal Regulatory Networks and an Abundance of Gene-Specific Repressors." *Cell* 157 (3): 740–52. doi:10.1016/j.cell.2014.02.054.

Kimura, Akatsuki, and Masami Horikoshi. 2004. "Partition of Distinct Chromosomal Regions: Negotiable Border and Fixed Border." *Genes to Cells*. doi:10.1111/j.1356-9597.2004.00740.x.

Kitada, T, B G Kuryan, N N Tran, C Song, Y Xue, M Carey, and M Grunstein. 2012. "Mechanism for Epigenetic Variegation of Gene Expression at Yeast Telomeric Heterochromatin." *Genes Dev* 26 (21): 2443–55. doi:10.1101/gad.201095.112.

Kitada, Tasuku, Thomas Schleker, Adam S. Sperling, Wei Xie, Susan M. Gasser, and Michael Grunstein. 2011. "??H2A Is a Component of Yeast Heterochromatin Required for Telomere Elongation." *Cell Cycle* 10 (2): 293–300. doi:10.4161/cc.10.2.14536.

Kristjuhan, A, B O Wittschieben, J Walker, D Roberts, B R Cairns, and J Q Svejstrup. 2003. "Spreading of Sir3 Protein in Cells with Severe Histone H3 Hypoacetylation." *Proc Natl Acad Sci U S A* 100 (13): 7551–56. doi:10.1073/pnas.1332299001332299100 [pii].

Lenstra, Tineke L., Joris J. Benschop, TaeSoo Kim, Julia M. Schulze, Nathalie A C H Brabers, Thanasis Margaritis, Loes A L van de Pasch, et al. 2011. "The Specificity and Topology of Chromatin Interaction Pathways in Yeast." *Molecular Cell* 42 (4): 536–49. doi:10.1016/j.molcel.2011.03.026.

Louis, EJ, and MM Becker. 2014. "Subtelomeres." http://link.springer.com/content/pdf/10.1007/978-3-642-41566-1.pdf.

Luo, K, M A Vega-Palas, and M Grunstein. 2002. "Rap1-Sir4 Binding Independent of Other Sir, yKu, or Histone Interactions Initiates the Assembly of Telomeric Heterochromatin in Yeast." *Genes Dev* 16 (12): 1528–39.

Maillet, L, C Boscheron, M Gotta, S Marcand, E Gilson, and S M Gasser. 1996. "Evidence for Silencing Compartments within the Yeast Nucleus: A Role for Telomere Proximity and Sir Protein Concentration in Silencer-Mediated Repression." *Genes Dev* 10 (14): 1796–1811. http://www.ncbi.nlm.nih.gov/pubmed/8698239.

Marcand, S, S W Buck, P Moretti, E Gilson, and D Shore. 1996. "Silencing of Genes at Nontelomeric Sites in Yeast Is Controlled by Sequestration of Silencing Factors at Telomeres by Rap 1 Protein." *Genes Dev.* 10 (11): 1297–1309.

Matsuda, Atsushi, Yuji Chikashige, Da-Qiao Ding, Chizuru Ohtsuki, Chie Mori, Haruhiko Asakawa, Hiroshi Kimura, Tokuko Haraguchi, and Yasushi Hiraoka. 2015. "Highly Condensed Chromatins Are Formed Adjacent to Subtelomeric and Decondensed Silent Chromatin in Fission Yeast." *Nature Communications* 6: 7753. doi:10.1038/ncomms8753.

Millar, Catherine B, and Michael Grunstein. 2006. "Genome-Wide Patterns of Histone Modifications in Yeast." *Nature Reviews. Molecular Cell Biology* 7 (9): 657–66. doi:10.1038/nrm1986.

Mitsumori, Risa, Tomoe Ohashi, Kazuto Kugou, Ayako Ichino, Kei Taniguchi, Kunihiro Ohta, Hiroyuki Uchida, and Masaya Oki. 2016. "Analysis of Novel Sir3 Binding Regions in Saccharomyces Cerevisiae." *Journal of Biochemistry* 160 (1): 11–17. doi:10.1093/jb/mvw021.

Moazed, D, A Kistler, A Axelrod, J Rine, and A D Johnson. 1997. "Silent Information Regulator Protein Complexes in Saccharomyces Cerevisiae: A SIR2/SIR4 Complex and Evidence for a Regulatory Domain in SIR4 That Inhibits Its Interaction with SIR3." *Proceedings of the National Academy of Sciences of the United States of America* 94 (6): 2186–91. doi:10.1073/pnas.94.6.2186.

Moretti, P, and D Shore. 2001. "Multiple Interactions in Sir Protein Recruitment by Rap1p at Silencers and Telomeres in Yeast." *Mol Cell Biol* 21 (23): 8082–94. doi:10.1128/MCB.21.23.8082-8094.2001.

Moretti, Paolo, Katie Freeman, Lavanya Coodly, and David Shore. 1994. "Evidence That a Complex of SIR Proteins Interacts with the Silencer and Telomere-Binding Protein RAP1." *Genes and Development* 8 (19): 2257–69. doi:10.1101/gad.8.19.2257.

Nakanishi, Shima, Shin Lee Jung, Kathryn E. Gardner, Jennifer M. Gardner, Yoh Hei Takahashi, Mahesh B. Chandrasekharan, Zu Wen Sun, et al. 2009. "Histone H2BK123 Monoubiquitination Is the Critical Determinant for H3K4 and H3K79 Trimethylation by COMPASS and Dot1." *Journal of Cell Biology* 186 (3): 371–77. doi:10.1083/jcb.200906005.

Nakayama, Jun-ichi, Amar J.S Klar, and Shiv I.S Grewal. 2000. "A Chromodomain Protein, Swi6, Performs Imprinting Functions in Fission Yeast during Mitosis and Meiosis." *Cell* 101 (3): 307–17. doi:10.1016/S0092-8674(00)80840-5.

Oki, Masaya, Lourdes Valenzuela, Tomoko Chiba, Takashi Ito, and Rohinton T Kamakaka. 2004. "Barrier Proteins Remodel and Modify Chromatin to Restrict Silenced Domains." *Molecular and Cellular Biology* 24 (5): 1956–67. doi:10.1128/MCB.24.5.1956-1967.2004.

Osborne, E A, S Dudoit, and J Rine. 2009. "The Establishment of Gene Silencing at Single-Cell Resolution." *Nat Genet* 41 (7): 800–806. doi:10.1038/ng.402.

Pelechano, Vicent, Sebastián Chávez, and José E. Pérez-Ortín. 2010. "A Complete Set of Nascent Transcription Rates for Yeast Genes." *PLoS ONE* 5 (11). doi:10.1371/journal.pone.0015442.

Peng, Jing, and Jin Qiu Zhou. 2012. "The Tail-Module of Yeast Mediator Complex Is Required for Telomere Heterochromatin Maintenance." *Nucleic Acids Research* 40 (2): 581–93. doi:10.1093/nar/gkr757.

Pryde, F E, and E J Louis. 1999. "Limitations of Silencing at Native Yeast Telomeres." *EMBO J* 18 (9): 2538–50.

Radman-Livaja, M, G Ruben, A Weiner, N Friedman, R Kamakaka, and O J Rando. 2011. "Dynamics of Sir3 Spreading in Budding Yeast: Secondary Recruitment Sites and Euchromatic Localization." *EMBO J* 30 (6): 1012–26. doi:10.1038/emboj.2011.30.

Renauld, H, O M Aparicio, P D Zierath, B L Billington, S K Chhablani, and D E Gottschling. 1993a. "Silent Domains Are Assembled Continuously from the Telomere and Are Defined by Promoter Distance and Strength, and by SIR3 Dosage." *Genes Dev* 7 (7A): 1133–45.

Renauld, H., O. M. Aparicio, P. D. Zierath, B. L. Billington, S. K. Chhablani, and D. E. Gottschling. 1993b. "Silent Domains Are Assembled Continuously from the Telomere and Are Defined by Promoter Distance and Strength, and by SIR3 Dosage." *Genes and Development* 7 (7 A): 1133–45. doi:10.1101/gad.7.7a.1133.

Rine, J., and I. Herskowitz. 1987. "Four Genes Responsible for a Position Effect on Expression from HML and HMR in Saccharomyces Cerevisiae." *Genetics* 116 (1): 9–22.

Robyr, D, Y Suka, I Xenarios, S K Kurdistani, A Wang, N Suka, and M Grunstein. 2002. "Microarray Deacetylation Maps Determine Genome-Wide Functions for Yeast Histone Deacetylases." *Cell* 109 (4): 437–46.

Roy, R, B Meier, A D McAinsh, H M Feldmann, and S P Jackson. 2004. "Separation-of-Function Mutants of Yeast Ku80 Reveal a Yku80p-Sir4p Interaction Involved in Telomeric Silencing." *J Biol Chem* 279 (1): 86–94.

Ruault, M, A De Meyer, I Loiodice, and A Taddei. 2011a. "Clustering Heterochromatin: Sir3 Promotes Telomere Clustering Independently of Silencing in Yeast." *J Cell Biol* 192 (3): 417–31. doi:jcb.201008007 [pii]10.1083/jcb.201008007.

———. 2011b. "Clustering Heterochromatin: Sir3 Promotes Telomere Clustering Independently of Silencing in Yeast." *J Cell Biol* 192 (3): 417–31. doi:10.1083/jcb.201008007.

Ruault, M, A De Meyer, I Loïodice, and A Taddei. n.d. "Clustering Heterochromatin: Sir3 Promotes Telomere Clustering Independently of Silencing in Yeast." *Journal of Cell Biology*.

Rudner, A D, B E Hall, T Ellenberger, and D Moazed. 2005. "A Nonhistone Protein-Protein Interaction Required for Assembly of the SIR Complex and Silent Chromatin." *Mol Cell Biol* 25 (11): 4514–28. doi:25/11/4514 [pii]10.1128/MCB.25.11.4514-4528.2005.

Rusche, L N, A L Kirchmaier, and J Rine. 2002. "Ordered Nucleation and Spreading of Silenced Chromatin in

Saccharomyces Cerevisiae." *Mol Biol Cell.* 7 (13): 2207–22.

Rusche, Laura N, Ann L Kirchmaier, and Jasper Rine. 2003. "The Establishment, Inheritance, and Function of Silenced Chromatin in Saccharomyces Cerevisiae." *Annual Review of Biochemistry* 72: 481–516. doi:10.1146/annurev.biochem.72.121801.161547.

Schulze, Julia M., Jessica Jackson, Shima Nakanishi, Jennifer M. Gardner, Thomas Hentrich, Jeff Haug, Mark Johnston, Sue L. Jaspersen, Michael S. Kobor, and Ali Shilatifard. 2009. "Linking Cell Cycle to Histone Modifications: SBF and H2B Monoubiquitination Machinery and Cell-Cycle Regulation of H3K79 Dimethylation." *Molecular Cell* 35 (5): 626–41. doi:10.1016/j.molcel.2009.07.017.

Sperling, A S, and M Grunstein. 2009. "Histone H3 N-Terminus Regulates Higher Order Structure of Yeast Heterochromatin." *Proc Natl Acad Sci U S A* 106 (32): 13153–59. doi:0906866106 [pii]10.1073/pnas.0906866106.

Strahl-Bolsinger, S, A Hecht, K Luo, and M Grunstein. 1997. "SIR2 and SIR4 Interactions Differ in Core and Extended Telomeric Heterochromatin in Yeast." *Genes Dev* 11 (1): 83–93. http://www.ncbi.nlm.nih.gov/entrez/query.fcgi?cmd=Retrieve&db=PubMed&dopt=Citation&list_uids=9000052.

Stulemeijer, Iris J. E., Dirk De Vos, Kirsten van Harten, Onkar K. Joshi, Olga Blomberg, Tibor van Welsem, Marit Terweij, et al. 2015. "Dot1 Histone Methyltransferases Share a Distributive Mechanism but Have Highly Diverged Catalytic Properties." *Scientific Reports* 5: 1–11. doi:10.1038/srep09824.

Taddei, A, G Van Houwe, F Hediger, V Kalck, F Cubizolles, H Schober, and S M Gasser. 2006. "Nuclear Pore Association Confers Optimal Expression Levels for an Inducible Yeast Gene." *Nature* 441 (7094): 774–78. doi:10.1038/nature04845.

Taddei, A, G Van Houwe, S Nagai, I Erb, E van Nimwegen, and S M Gasser. 2009. "The Functional Importance of Telomere Clustering: Global Changes in Gene Expression Result from SIR Factor Dispersion." *Genome Res* 19 (4): 611–25. doi:gr.083881.108 [pii]10.1101/gr.083881.108.

Tadeo, Xavier, Jiyong Wang, Scott P. Kallgren, Jinqiang Liu, Bharat D. Reddy, Feng Qiao, and Songtao Jia. 2013. "Elimination of Shelterin Components Bypasses RNAi for Pericentric Heterochromatin Assembly." *Genes and Development* 27 (22): 2489–99. doi:10.1101/gad.226118.113.

Talbert, Paul B, and Steven Henikoff. 2006. "Spreading of Silent Chromatin: Inaction at a Distance." *Nature Reviews. Genetics* 7 (10): 793–803. doi:10.1038/nrg1920.

Thompson, J S, L M Johnson, and M Grunstein. 1994. "Specific Repression of the Yeast Silent Mating Locus HMR by an Adjacent Telomere." *Mol Cell Biol* 14 (1): 446–55.

Thompson, J S, X Ling, and M Grunstein. 1994. "Histone H3 Amino Terminus Is Required for Telomeric and

Silent Mating Locus Repression in Yeast." *Nature* 369: 245–47. doi:10.1038/369245a0.

Triolo, T, and R Sternglanz. 1996. "Role of Interactions between the Origin Recognition Complex and SIR1 in Transcriptional Silencing." *Nature* 381 (6579): 251–53.

Tsukamoto, Y, J-I Kato, and H Ikeda. 1997. "Silencing Factors Participate in DNA Repair and Recombination in Saccharomyces Cerevisiv¶." *Nature* 388: 900–903.

Van De Vosse, David W., Yakun Wan, Diego L. Lapetina, Wei Ming Chen, Jung Hsien Chiang, John D. Aitchison, and Richard W. Wozniak. 2013. "A Role for the Nucleoporin Nup170p in Chromatin Structure and Gene Silencing." *Cell* 152 (5): 969–83. doi:10.1016/j.cell.2013.01.049.

Venkatasubrahmanyam, S, W W Hwang, M D Meneghini, A H Tong, and H D Madhani. 2007. "Genome-Wide, as Opposed to Local, Antisilencing Is Mediated Redundantly by the Euchromatic Factors Set1 and H2A.Z." *Proc Natl Acad Sci U S A* 104 (42): 16609–14. http://www.ncbi.nlm.nih.gov/entrez/query.fcgi?cmd=Retrieve&db=PubMed&dopt=Citation&list_uids=17925448.

Verzijlbergen, Kitty F, Alex W Faber, Iris Je Stulemeijer, and Fred van Leeuwen. 2009. "Multiple Histone Modifications in Euchromatin Promote Heterochromatin Formation by Redundant Mechanisms in Saccharomyces Cerevisiae." *BMC Molecular Biology* 10: 76. doi:10.1186/1471-2199-10-76.

Wang, F, G Li, M Altaf, C Lu, M A Currie, A Johnson, and D Moazed. 2013. "Heterochromatin Protein Sir3 Induces Contacts between the Amino Terminus of Histone H4 and Nucleosomal DNA." *Proc Natl Acad Sci U S A* 110 (21): 8495–8500. doi:10.1073/pnas.1300126110.

Wang, Xiaorong, Jessica J. Connelly, Chia Lin Wang, and Rolf Sternglanz. 2004. "Importance of the Sir3 N Terminus and Its Acetylation for Yeast Transcriptional Silencing." *Genetics* 168 (1): 547–51. doi:10.1534/genetics.104.028803.

Weiner, A, T H Hsieh, A Appleboim, H V Chen, A Rahat, I Amit, O J Rando, and N Friedman. 2015. "High-Resolution Chromatin Dynamics during a Yeast Stress Response." *Mol Cell* 58 (2): 371–86. doi:10.1016/j.molcel.2015.02.002.

Yue, Jia-Xing, Jing Li, Louise Aigrain, Johan Hallin, Karl Persson, Karen Oliver, Anders Bergström, et al. 2017. "Contrasting Evolutionary Genome Dynamics between Domesticated and Wild Yeasts." *Nature Genetics* 49 (6): 913–24. doi:10.1038/ng.3847.

Strain table

ID	matingT.	genotype	background
191	alpha	ade2-1::ADE2 adh4::URA3-4xUASG-(C1-3A)n ppr1Δ::HIS3 rap1::GFP-RAP1(LEU2)	(W303)
1254	alpha	ade2-1::ADE2 adh4::URA3-4xUASG-(C1-3A)n ppr1Δ::HIS3 rap1::GFP-RAP1(LEU2) sir3::GPD-SIR3(NAT)	(W303)
1256	alpha	ade2-1::ADE2 adh4::URA3-4xUASG-(C1-3A)n ppr1Δ::HIS3 rap1::GFP-RAP1(LEU2) sir3::GPD-sir3-A2Q(NAT)	(W303)
2487	a	ade2-1::ADE2 hmlΔ::HPH rap1::RAP1-GFP(LEU2)	(W303)
2627	a	ade2-1::ADE2 hmlΔ::HPH rap1::RAP1-GFP(LEU2) sir3::pADH-SIR3(NAT)	(W303)
2629	a	ade2-1::ADE2 hmlΔ::HPH rap1::RAP1-GFP(LEU2) sir3::pTEF-SIR3(NAT)	(W303)
2554	a	ade2-1::ADE2 hmlΔ::HPH rap1::RAP1-GFP(LEU2) sir3::GPD-Sir3(NAT)	(W303)
1667	a	RAD5+ rap1::RAP1-GFP(LEU2) RDN1::ADE2 sir2::GPD-SIR2(KanMX)	(W303)
1668	a	RAD5+ rap1::RAP1-GFP(LEU2) RDN1::ADE2 sir2::GPD-SIR2(KanMX)sir3::GPD-SIR3(NAT)	(W303)
779	a	ade2-1::ADE2 sir3::SIR3-GFP(LEU2)	(W303)
3441	a	ade2-1::ADE2 sir3::(KAN) pADH-SIR3-GFP(LEU2)	(W303)
3442	a	ade2-1::ADE2 sir3::(KAN)pTEF-SIR3-GFP(LEU2)	(W303)
3443	a	ade2-1::ADE2 sir3::(KAN) pGPD-SIR3-GFP(LEU2)	(W303)
2056	a	can1::MFA1pr-HIS3 hht1-hhf1::NatMX4 hht2-hhf2::[HHTS-HHFS]*-URA3 where H4WT	BY4733
2986	a	can1::MFA1pr-HIS3 hht1-hhf1::NatMX4 hht2-hhf2::[HHTS-HHFS]*-URA3 where H3Δ4-30 Rap1-GFP(LEU2)	BY4733
2987	a	can1::MFA1pr-HIS3 hht1-hhf1::NatMX4 hht2-hhf2::[HHTS-HHFS]*-URA3 where H3Δ4-30 Rap1-GFP(LEU2) pGPD-SIR3(NAT)	BY4733
2476	a	rap1::GFP-RAP1(LEU2) sir3::GPD-SIR3(NAT)	BY4741

3004	alpha	ade2-1::ADE2 adh4::URA3-4xUASG-(C1-3A)n ppr1Δ::HIS3 rap1::GFP-RAP1(LEU2) bre1Δ::KanMx	(W303)
3123	alpha	ade2-1::ADE2 adh4::URA3-4xUASG-(C1-3A)n ppr1Δ::HIS3 rap1::GFP-RAP1(LEU2) bre1Δ::KanMx SIR3::pGPD-SIR3 (NatMx)	(W303)
3180	alpha	ade2-1::ADE2 adh4::URA3-4xUASG-(C1-3A)n ppr1Δ::HIS3 rap1::GFP-RAP1(LEU2) dot1Δ::KanMx	(W303)
3181	alpha	ade2-1::ADE2 adh4::URA3-4xUASG-(C1-3A)n ppr1Δ::HIS3 rap1::GFP-RAP1(LEU2) set1Δ::KanMx	(W303)
3182	alpha	ade2-1::ADE2 adh4::URA3-4xUASG-(C1-3A)n ppr1Δ::HIS3 rap1::GFP-RAP1(LEU2) dot1Δ::KanMx pGPD-SIR3-A2Q (NAT)	(W303)
3183	alpha	ade2-1::ADE2 adh4::URA3-4xUASG-(C1-3A)n ppr1Δ::HIS3 rap1::GFP-RAP1(LEU2) dot1Δ::KanMx pGPD-SIR3 (NAT)	(W303)
3184	alpha	ade2-1::ADE2 adh4::URA3-4xUASG-(C1-3A)n ppr1Δ::HIS3 rap1::GFP-RAP1(LEU2) set1Δ::KanMx pGPD-SIR3(NAT)	(W303)
2838	alpha	ade2-1::ADE2 adh4::URA3-4xUASG-(C1-3A)n ppr1Δ::HIS3 rap1::GFP-RAP1(LEU2) rpd3Δ::KanMx	(W303)
2841	alpha	ade2-1::ADE2 adh4::URA3-4xUASG-(C1-3A)n ppr1Δ::HIS3 rap1::GFP-RAP1(LEU2) rpd3Δ::KanMx pGPD-SIR3(NAT)	(W303)
3301	1N	ade2-1::ADE2 adh4::URA3-4xUASG-(C1-3A)n ppr1Δ::HIS3 rap1::GFP-RAP1(LEU2) set2Δ::(KanMx)	(W303)
3333	1N	ade2-1::ADE2 adh4::URA3-4xUASG-(C1-3A)n ppr1Δ::HIS3 rap1::GFP-RAP1(LEU2) set2Δ::(KanMx) sir3::GPD-SIR3(NAT)	(W303)

Supplementary figures

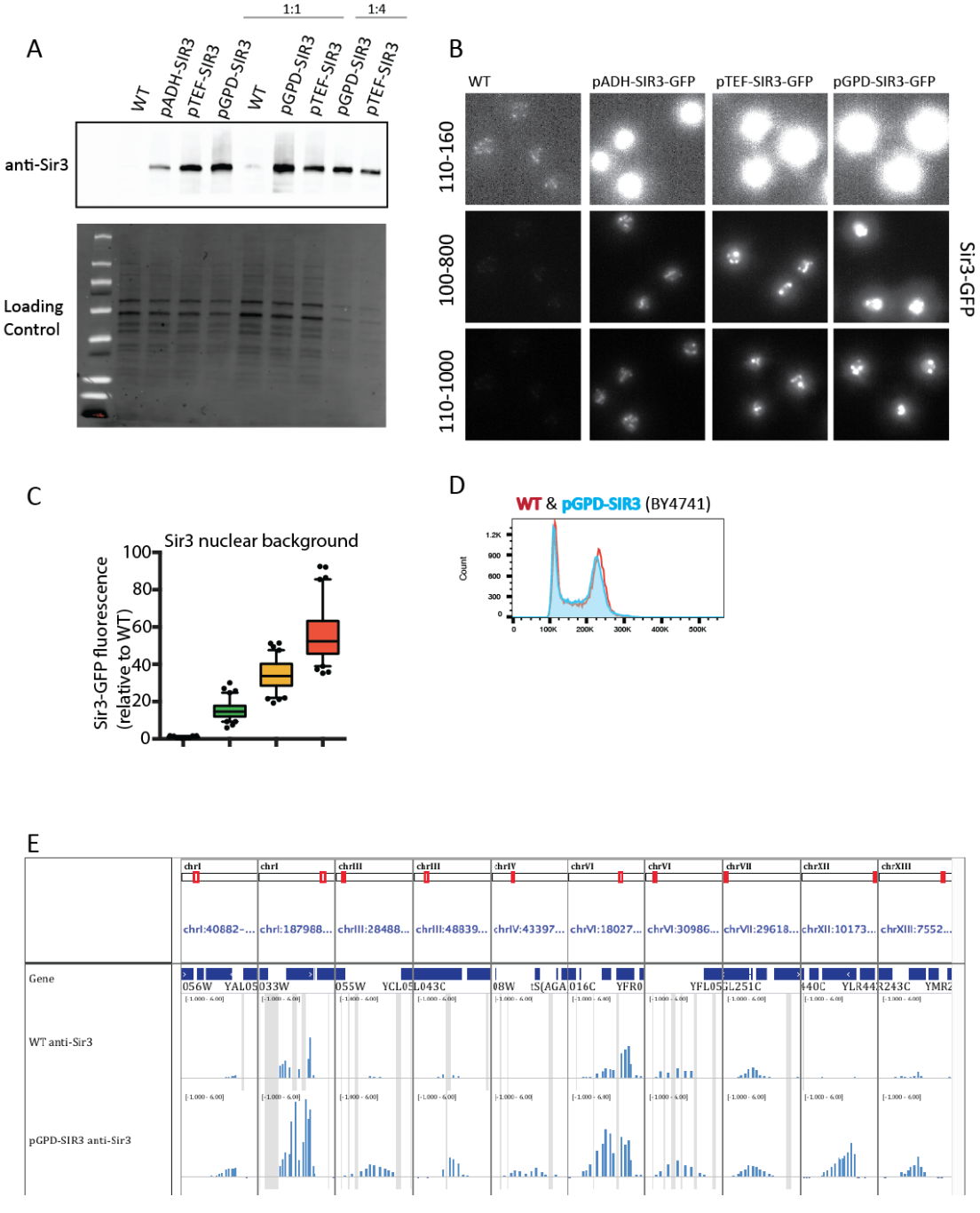

Supplementary Figure 1 (A) Western Blot anti-Sir3 in the strains used in Figure one for ChIP-chip. (B) representative examples of Sir3 fluorescence in strains overexpressing Sir3-GFP (C) Quantification of Sir3-GFP nuclear background (D) FACS profile of exponentially growing WT and pGPD-SIR3 strains (E) Representative images of loci bound by Sir3 within euchromatin.

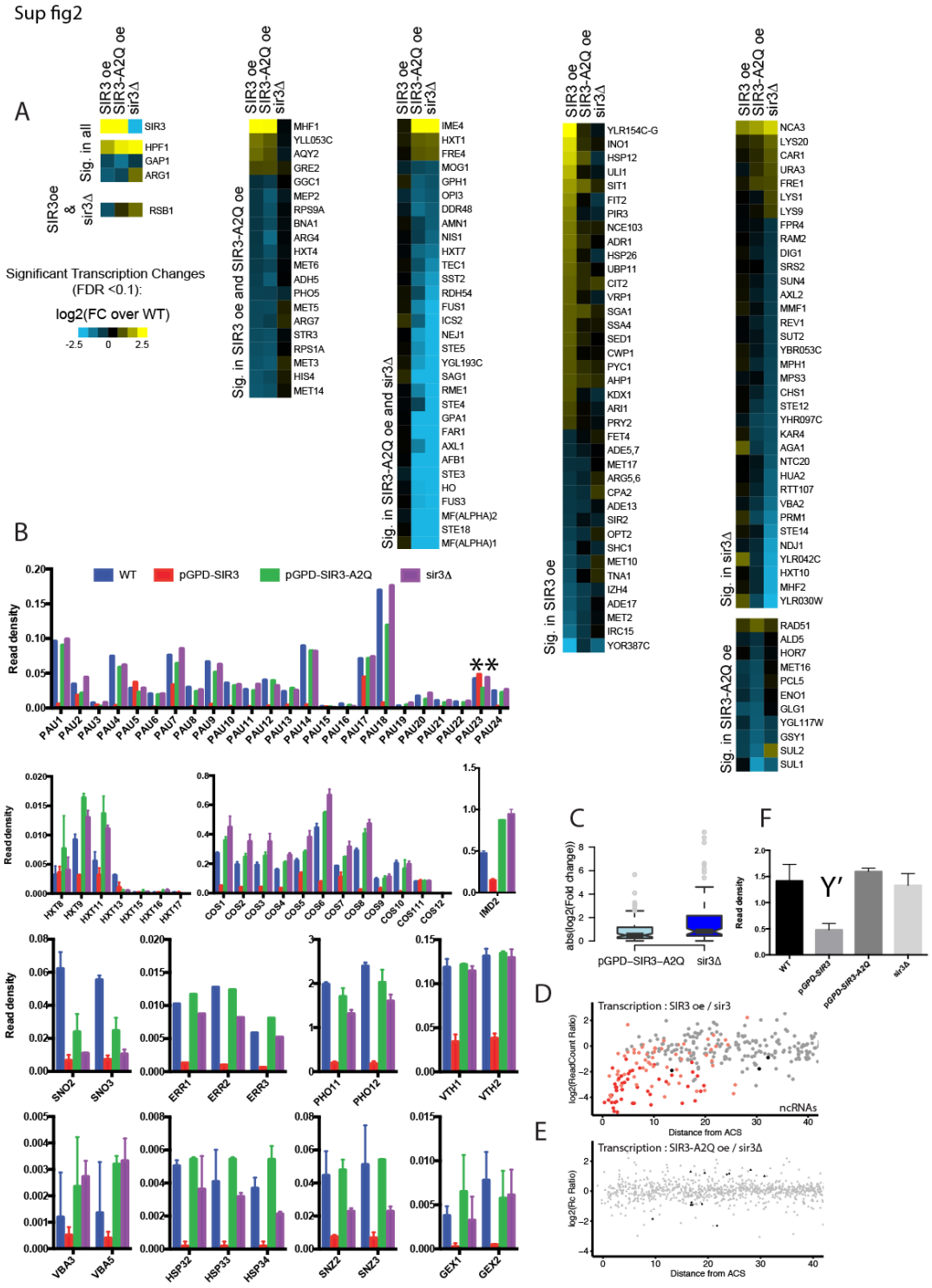

Supplementary Figure 2 : (A) All transcriptional changes coined significant by EdgeR within euchromatin, color code indicate log2(FC). (B) Transcriptional changes of genes from subtelomeric families.(C) absolute fold change of genes associated to pseudo-diploid signature.(D) Transcription of ncRNA within subtelomere, color code is identical as in the main figure.(E) Transcriptional changes in SIR3-A2Q mutants versus sir3 mutants. (F) Average Read density at Y' elements.

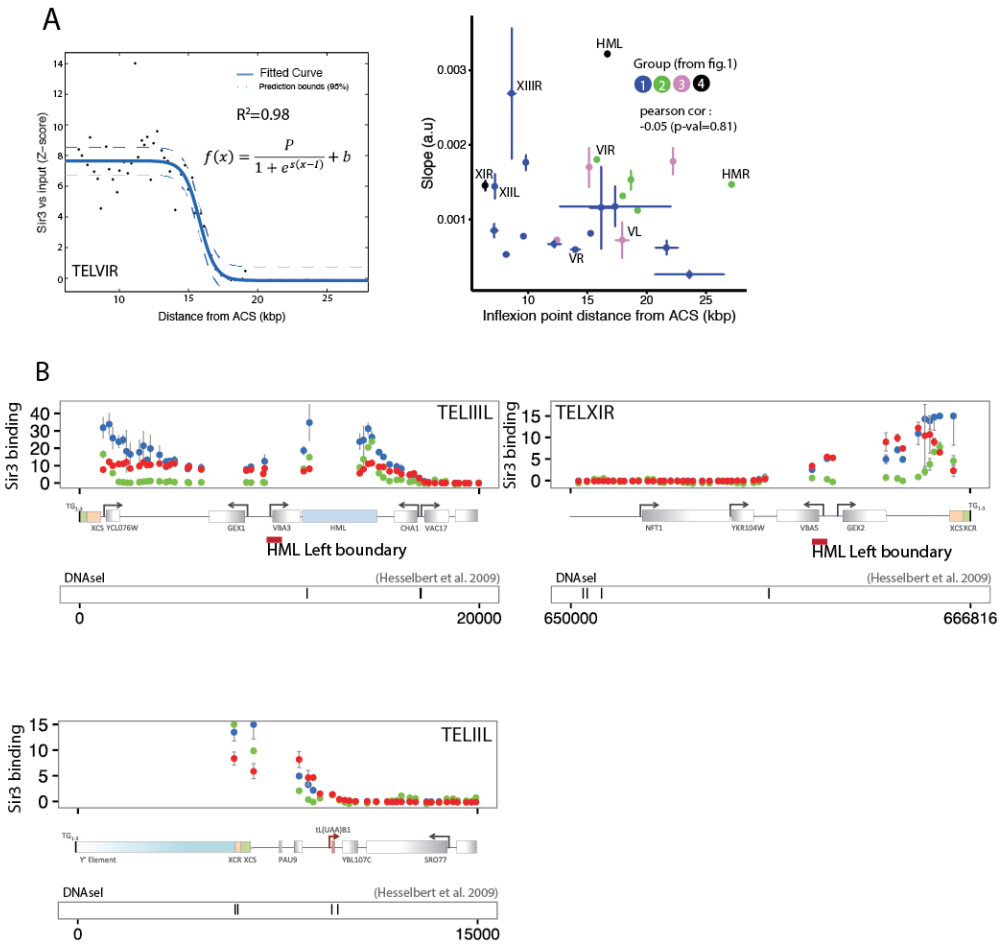

C

Transcription factor binding at extended silent domains

Transcription factor	Location			Data source
	Within E.S.D	"-1Gene"	"+1Gene"	
Abf1	3	2	2	H
Adr1	5	2	1	H
Gcn4	5	2	1	H
Hsf1	1	0	1	H
Leu3	0	0	0	H
Rap1	7	1	1	R
Reb1	3	2	2	R
|	1	0	1	H
Rgt1	0	0	0	H
Sfp1	0	0	0	H
Swi5	23 (10 Y', 3 COS)	1	0	H
Tbf1	1	2	1	P

H: Harbison et al., 2004; P: Preti et al., 2010; R: Rhee et al., 2011

Transcription factor binding at end of extended silent domains

Gene name	Gene position		Telomere	Data source
	-1	1		
YBR293W	Abf1		IIR	*H*
iYBR292C-1		Abf1		*H*
iYCR095C-0	Adr1		IIIR	*H*
iYCR095C-1	Gcn4			*H*
YCR095C	Reb1			*R*
YCR094W		Reb1		*H;R*
YDL240W		Rap1	IVL	*R*
YFL051C	Tbf1		VIL	*P*
YFL051C	Rap1			*R*
YFR052W		Reb1	VIR	*R*
iYGL254W	Abf1		VIIL	*H*
YGL253W		Abf1		*H*
YHL041W	Tbf1		VIIIL	*P*
YKL217W	Reb1		XIL	*R*
YML131W	Swi5		XIIIL	*H*
YMR319C		Tbf1	XIIIR	*P*
iYPL274W		Gcn4	XVIL	*H*
iYOL154W	Gcn4		XVL	*H*
iYOR387C-0	Adr1		XVR	*H*

H: Harbison et al., 2004; P: Preti et al., 2010; R: Rhee et al., 2011

Supplementary Figure 3: (A) Example of fitting of the ChIP-chip data, function used is shown on the graph. Right: Inferred slope versus position of inflexion point. (B) Examples of identified barrier at three subtelomeres at which Sir3 spreading does not extent when Sir3 dosage is increased. (C) List of transcription factors possessing a barrier property and present within E.S.D (left) or at the boundary of E.S.D (right)

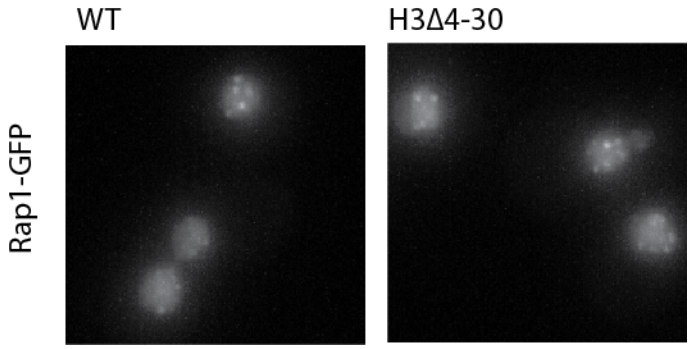

Supplementary Figure 4 : Maximal projections of Rap1-GFP images in WT and H3Δ4-30 strain, grown to exponential phase

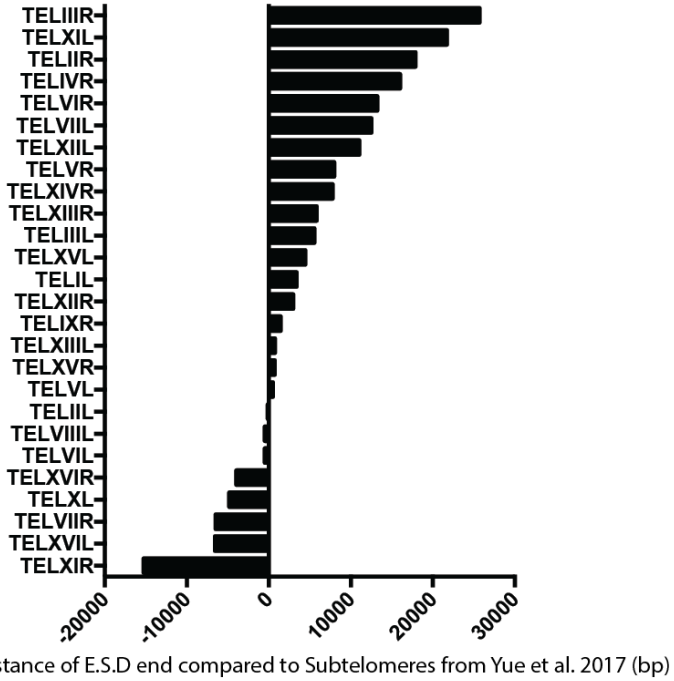

Supplementary Figure 5: Comparison of the location of the End of extended silent domains with subtelomeres ends as defined by (Yue et al. 2017) Positive distance implies that the E.S.D end further within the core chromosome that the subtelomere as defined by synteny.

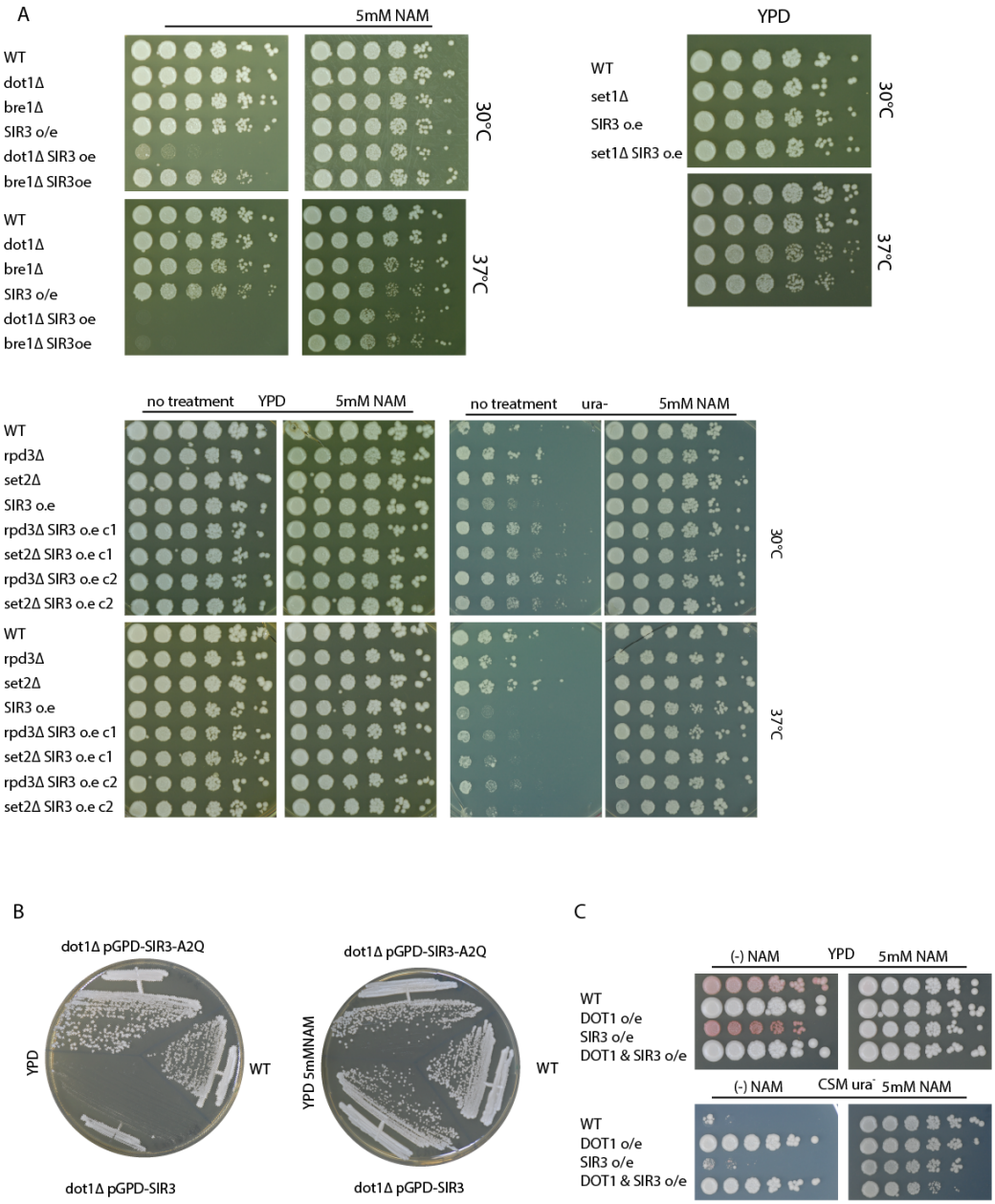

Supplementary Figure 6 (A) Drop assays probing viability in the presence of absence of 5mM NAM. Protocol is identical to the one shown on the main figure. (B) dot1 mutants overexpressing Sir3-A2Q are viable.(C) Dot1 overexpression counteracts Sir3 overexpression.